Free Radical Biology and Medicine 189 (2022) 111–121

Contents lists available at ScienceDirect

Free Radical Biology and Medicine

journal homepage: www.elsevier.com/locate/freeradbiomed

GSNOR deficiency attenuates MPTP-induced neurotoxicity and autophagy by facilitating CDK5 *S*-nitrosation in a mouse model of Parkinson's disease

Lijin Jiao [a,b,1], Ling-Yan Su [a,b,1], Qianjin Liu [a,b,1], Rongcan Luo [a,b], Xinhua Qiao [c], Ting Xie [c], Lu-Xiu Yang [a], Chang Chen [c], Yong-Gang Yao [a,b,d,*]

[a] *Key Laboratory of Animal Models and Human Disease Mechanisms of the Chinese Academy of Sciences & Yunnan Province, and KIZ-CUHK Joint Laboratory of Bioresources and Molecular Research in Common Diseases, Kunming Institute of Zoology, Kunming, Yunnan, 650204, China*

[b] *Kunming College of Life Science, University of Chinese Academy of Sciences, Kunming, Yunnan, 650204, China*

[c] *National Laboratory of Biomacromolecules, CAS Center for Excellence in Biomacromolecules, Institute of Biophysics, Chinese Academy of Sciences, Beijing, 100101, China*

[d] *CAS Center for Excellence in Brain Science and Intelligence Technology, Chinese Academy of Sciences, Shanghai, 200031, China*

ARTICLE INFO

Keywords:
Autophagy
CDK5
GSNOR
Parkinson's disease
S-nitrosation

ABSTRACT

The *S*-nitrosoglutathione reductase (GSNOR) is a key denitrosating enzyme that regulates protein *S*-nitrosation, a process which has been found to be involved in the pathogenesis of Parkinson's disease (PD). However, the physiological function of GSNOR in PD remains unknown. In a 1-methyl-4-phenyl-1,2,3,6-tetrahydropyridine (MPTP)-induced PD mouse model, we found that GSNOR expression was significantly increased and accompanied by autophagy mediated by MPTP-induced cyclin dependent kinase 5 (CDK5), behavioral dyskinesias and dopaminergic neuron loss. Whereas, knockout of GSNOR, or treatment with the GSNOR inhibitor N6022, alleviated MPTP-induced PD-like pathology and neurotoxicity. Mechanistically, deficiency of GSNOR inhibited MPTP-induced CDK5 kinase activity and CDK5-mediated autophagy by increasing *S*-nitrosation of CDK5 at Cys83. Our study indicated that GSNOR is a key regulator of CDK5 *S*-nitrosation and is actively involved in CDK5-mediated autophagy induced by MPTP.

1. Introduction

Parkinson's disease (PD) is a complex neurodegenerative disease characterized by progressive depletion of dopamine (DA) in the substantia nigra pars compacta (SNc) and the presence of intraneuronal Lewy body aggregates [1,2]. The clinical manifestations of PD include static tremor, muscle stiffness, bradykinesia, and disorders of balance [1,2]. Accumulating evidence suggests that genetic factors [3,4], mitochondrial dysfunction [5,6] and neuroinflammation [7,8] each play an important role in the development of PD. However, the exact mechanisms of PD are insufficiently understood and this hinders the treatment of PD.

The *S*-nitrosation of proteins, a covalent reaction of nitric oxide-related species with a cysteine thiol group to form *S*-nitrosothiol, can be a pivotal modulator of signal transduction pathways and a normal physiological response of the organism [9–11]. In recent years, the *S*-nitrosation of proteins has been reported to be associated with PD progression, with conflicting evidence showing a neuro-protective and a neuro-destructive role in animal models and PD patients [12–16]. The *S*-nitrosoglutathione reductase (GSNOR), which is encoded by the alcohol dehydrogenase 5 (*ADH5* or *GSNOR*) gene and modulates denitrosation of proteins, is widely present in prokaryotes and eukaryotes [17]. There are many studies showing an active involvement of GSNOR in a variety of diseases [18–22]. For instance, we found that GSNOR facilitated antiviral innate immunity by restricting *S*-nitrosation of TANK-binding kinase 1 [23], and during aging increased GSNOR expression impairs cognitive function and decreases *S*-nitrosation of CAMK2A (calcium/calmodulin-dependent protein kinase II alpha) [24]. Also, knockdown of GSNOR protected SH-SY5Y cells from 1-Methyl-4--phenylpyridinium (MPP^+, a metabolite of MPTP)-induced toxicity [25].

In the present study, we hypothesized that the GSNOR-mediated denitrosation played a pivotal role in the development of PD and

* Corresponding author. Key Laboratory of Animal Models and Human Disease Mechanisms of the Chinese Academy of Sciences & Yunnan Province, and KIZ-CUHK Joint Laboratory of Bioresources and Molecular Research in Common Diseases, Kunming Institute of Zoology, Kunming, Yunnan, 650204, China.
E-mail address: yaoyg@mail.kiz.ac.cn (Y.-G. Yao).

[1] These authors contributed equally to this work.

https://doi.org/10.1016/j.freeradbiomed.2022.07.016
Received 15 May 2022; Received in revised form 14 June 2022; Accepted 19 July 2022
Available online 30 July 2022

aimed to perform an in-depth exploration of the underpinning of GSNOR in the disease. By using mouse and cellular models of PD induced by MPTP or its derivate MPP^+, we demonstrated that GSNOR is actively involved in PD, and uncovered the underlying mechanism that knockout or inhibition of GSNOR enhanced *S*-nitrosation of cyclin dependent kinase 5 (CDK5) and inhibited CDK5 kinase activity, resulting in an attenuation of CDK5-mediated autophagy and neurotoxicity induced by MPTP. Our findings suggested that GSNOR is a key regulator in the PD mouse model and may represent a therapeutic target for the prevention and treatment of this important disease.

2. Materials and methods

2.1. Antibodies, reagents and cells

The antibodies and reagents used in this study are listed in Table S1. Rat C6 cells and PC12 cells were supplied by the Kunming Cell Bank, Kunming Institute of Zoology (KIZ), Chinese Academy of Sciences (CAS). Cells were cultured in Dulbecco's modified Eagle's medium (DMEM) medium (Gibco-BRL, 11965–092) with 10% fetal bovine serum (Gibco-BRL, 10099–141) and 1 × penicillin/streptomycin (Gibco, 15140122) at 37 °C in 5% CO_2.

2.2. Vector construction and transfection

Expression vector for rat GSNOR was purchased from the Miaoling Plasmid Sharing Platform (MLPSP). We amplified rat *Cdk5* coding region using a pair of gene-specific primers (Table S2), with complementary DNA (cDNA) prepared from the C6 cells as the template. The PCR product of *Cdk5* was purified with TIANquick Midi Purification Kit (Tiangen, DP204) and cloned into pCS2-N-Myc (pCS2-N-Myc-CDK5) using ClonExpress® IIOne Step Cloning Kit (Vazyme; C112) to make an expression vector for rat CDK5 with Myc-label (Myc-CDK5-WT). Site-directed mutageneses of eight cysteine residues in rat CDK5 protein (p.C53S, p.C83S, p.C94S, p.C117S, p.C157S, p.C190S, p.C269S and p.C290S) were performed using eight pairs of primers (Table S2) designed to substitute the respective cysteine residue with serine residue by using the Easy Mutagenesis System (Beijing TransGen Biotech) according to the manufacturer's protocols. All constructs were confirmed by Sanger sequencing.

The transient transfection of vectors was performed using Lipofectamine™ 3000 (Invitrogen, L3000015) according to the manufacturer's protocols. Briefly, cells were seeded on either 6-well plates or 10 cm cell culture dishes. When cells are 50%–60% confluent, growth medium was removed and cells were washed once with Opti-MEM medium (Gibco-BRL, 31985–070) for transfection. Expression vectors or empty vector (2.5 μg/well or 10 μg/dish) were dissolved in Opti-MEM medium (125 μL/well or 500 μL/dish) containing P3000™ regent (5 μL/well or 20 μL/dish), then were mixed with Lipofectamine™ 3000 (3.75 μL/well or 15 μL/dish) diluted in Opti-MEM medium (125 μL/well or 500 μL/dish). The mixture was incubated at room temperature for 15 min, and added to each well or dish together with an additional Opti-MEM medium (750 μL/well or 3000 μL/dish). The medium was removed at 6 h after transfection and fresh growth medium (2 mL/well or 8 mL/dish) was added for growth until harvest at 48 h after transfection.

2.3. CRISPR/Cas9-mediated knockout of Gsnor in C6 and PC12 cells

We created GSNOR knockout C6 and PC12 cells by using a CRISPR/Cas9 procedure described in our previous study [26]. Briefly, small guide RNAs (sgRNAs) (*Gsnor*-sgRNA-forward: CACCGGTGTAAGGCTGCAGTCGCC/*Gsnor*-sgRNA-reverse: AAACGGCGACTGCAGCCTTACACC) targeting *Gsnor* were annealed and cloned into the pX330-T7 vector expressing mCherry. The C6 and PC12 cells were transfected with the pX330-T7 vector carrying the sgRNAs using Lipofectamine™ 3000 (Invitrogen, L3000015). We sorted the transfected cells expressing mCherry by flow cytometry, followed by a culture for 48 h, then single cells were manually picked with a mouth pipette for expansion for 3 weeks. The genomic DNA of the expanded single cells was extracted using an AxyPrep Multisource Genomic DNA Miniprep Kit (Axygen, 26817KC1). The gene region spanning the sgRNA targeting site was amplified using primer pair *Gsnor*-F: TTGCTCCACCATGTATCGA/*Gsnor*-R: CCTTCTCCCACAATGCTTA, and cloned into T-Vector pMD19 (Takara, 6013). About 10 clones were randomly picked for sequencing validation. The successful knockout of the endogenous GSNOR protein was further confirmed by Western blot.

2.4. Western blot

Western blot assays for the target proteins were performed using the common approach as described in our previous studies [27,28]. Briefly, cell lysates of mouse brain tissues, and rat C6 and PC12 cells were prepared, and protein concentration was determined by BCA protein assay kit (Beyotime Institute of Biotechnology, P0012). We used around 25 μg of protein per sample for each assay. Next the protein was separated using 12% or 15% sodium dodecyl sulphate-polyacrylamide gel electrophoresis (SDS-PAGE) and transferred to a polyvinylidene difluoride membrane (BioRad, L1620177 Rev D), the membrane was soaked with 5% (w/v) skim milk for 2 h at room temperature, then was incubated with primary antibody (Table S1) overnight at 4 °C. The membrane was washed 3 times with TBST (Tris-buffered saline [Servicebio, G0001] with 0.1% Tween 20 [Sigma, P1379]), each time 5 min, followed by incubation with the secondary antibody. Peroxidase-conjugated anti-mouse (lot number 474–1806) or anti-rabbit (lot number 474–1516) IgG (1:10000; KPL) were used as the respective secondary antibodies. The epitope was visualized using an ECL Western Blot Detection Kit (Millipore, WBKLS0500). We used ImageJ (National Institutes of Health, Bethesda, Maryland, USA) to evaluate densitometry of each blot.

2.5. The biotin switch assay

The *S*-nitrosation modification of protein was detected as previously described [29,30]. Briefly, cells and brain tissue samples were homogenized in HEN buffer (250 mM HEPES-NaOH [pH 7.7], 1 mM EDTA, and 0.1 mM neocuproine) with 1% (v/v) NP-40. The free cysteine thiols were blocked with blocking buffer (2.5% SDS, 20 mM Methyl methanethiosulfonate [MMTS (Sigma-Aldrich, 208795-1G)] in HEN buffer) at 50 °C for 30 min with frequent vortexing, excess MMTS was removed by ice-cold acetone precipitation for 30 min, followed by centrifugation at 2000×*g* for 10 min at 4 °C. This precipitation was repeated three times to remove the residual MMTS. The protein pellet was suspended in HENS buffer (250 mM HEPES-NaOH [pH 7.7], 1 mM EDTA, 0.1 mM neocuproine, and 1% SDS) with 0.4 mM sulfhydryl-specific biotinylating reagent N-(6-(biotinamido) hexyl)-30-(20-pyridyldithio) propionamide (biotin-HPDP) and 10 mM ascorbate, and incubated for 2 h at room temperature. The excess biotin-HPDP was removed by ice-cold acetone precipitation for 30 min followed by centrifugation at 2000×*g* for 10 min at 4 °C. The protein pellet was suspended in HENS buffer, streptavidin-agarose beads and three volumes of neutralization buffer (20 mM HEPES-NaOH [pH 7.7], 100 mM NaCl, 1 mM EDTA, 0.5% Triton X-100) were added and incubated overnight at 4 °C. Beads were then washed 5 times with neutralization buffer with 0.6 M NaCl and eluted by elution buffer (20 mM HEPES-NaOH [pH 7.7], 100 mM NaCl, 1 mM EDTA, 100 mM β-Mercaptoethanol). The eluted mixture was analyzed by SDS-PAGE. The composition of the buffer used in these assays is shown in Table S3.

2.6. CDK5 activity assay

The CDK5 kinase assay was performed as previously described [31]. In brief, brain tissue or cell samples were homogenized in ice-cold lysis

buffer (Beyotime Institute of Biotechnology, P0013) for 1 h, followed by centrifugation at 12000×*g* for 10 min at 4 °C. The protein concentration was quantified by BCA protein assay kit (Beyotime Institute of Biotechnology, P0012). The anti-CDK5 antibody (for endogenous CDK5 activity assay) or anti-Myc antibody (for exogenously expressed CDK5 activity assay in cultured cells) were incubated with protein G-agarose beads (Life Technologies, 15920010) to form a complex for 2 h at room temperature, followed by adding 300 μg protein and an incubation overnight at 4 °C. The immunoprecipitate was washed 5 times with lysis buffer, and suspended in a volume of 20 μL of the assay dilution buffer (100 mM MOPS, pH 7.2, 125 mM β-glycerophosphate, 25 mM EGTA, 5 mM sodium orthovanadate, 5 mM dithiothreitol) containing 100 μM ATP, then 1 μg of recombinant Histone H1 protein (as the substrate of CDK5) was added for reaction at 30 °C for 30 min. The phosphorylated Histone H1 protein was separated by 15% SDS-PAGE and immunoblotted with specific anti-phospho-histone H1 antibody.

2.7. Confocal microscopy assay

Cultured C6 and PC12 cells (wild type and *Gsnor*$^{-/-}$ cells) were co-transfected with N-terminally tagged pEGFP-C1-LC3 [28] and with empty vector (Vector-flag) or N-terminally tagged pEGFP-C1-LC3 and GSNOR (Gsnor-Flag) for 24 h, then received MPTP (500 μM, for C6 cells) or MPP^+ (100 μM, for PC12 cells) treatment for another 24 h before being imaged by the confocal microscopy, followed the same procedure as described in our previous study [28]. Briefly, cells were fixed with 4% paraformaldehyde for 10 min, followed by three washes with phosphate-buffered saline (PBS, pH 7.4; each 3 min). Cells were then permeabilized with PBS with Triton X-100 0.1% (Beyotime Institute of Biotechnology, C0221A) for 4 min at room temperature. After another round of three washes with PBS, nuclei were stained with 1 μg/mL DAPI (Roche Diagnostics, 10236276001) for 10 min, followed by a third round of three washes with PBS. Cells were imaged under an Olympus FluoView™ 1000 confocal microscope (Olympus, America).

2.8. Animals, drug treatment and behavioral tests

The *Gsnor*$^{-/-}$ mice on a C57BL/6 J background were described in our previous studies [23,24]. Animals were kept in specific pathogen-free animal house at the Experimental Animal Center of KIZ, with free access to water and food at 22 ± 2 °C, 50% humidity, and a 12 h light/dark cycle. All animal experimental procedures and protocols were approved by the Institutional Review Board of KIZ, CAS.

For drug treatments, MPTP was dissolved in 0.9% saline, and the GSNOR inhibitor N6022 was dissolved in saline with 0.5% dimethylsulfoxide (DMSO) (v/v), and saline with 0.5% DMSO was used as a vehicle. We treated *Gsnor*$^{-/-}$ and wild type (WT) male mice (8–10 weeks old) with or without MPTP (30 mg/kg), following the protocol described in our previous study [28]. Briefly, animals of each genotype were divided into two groups and were subcutaneously injected with MPTP (MPTP group: WT MPTP group, n = 10; *Gsnor*$^{-/-}$ MPTP group, n = 9) or equivalent volume of 0.9% saline (saline group: WT saline group, n = 8; *Gsnor*$^{-/-}$ saline group, n = 8) daily for 14 days. The animals were subjected to behavioral tests including the rota rod task, traction test and pole test on day 15. After the behavioral tests, animals were euthanized with pentobarbital for tissue collection. In order to evaluate potential prevention effect of N6022 against the toxicity of MPTP in WT mice (8–10 weeks old), N6022 (5 mg/kg) or vehicle was injected intraperitoneally 30 min before subcutaneous injection of MPTP (30 mg/kg) or saline. Briefly, animals were divided into four groups for the respective treatment daily for 14 days: (1) Vehicle + saline group (n = 8), mice were injected with vehicle and saline; (2) Vehicle + MPTP group (n = 8), mice were injected with vehicle and MPTP; (3) N6022+saline group (n = 8), mice were injected with N6022 and saline; and (4) N6022+MPTP group (n = 8), mice were injected with N6022 and MPTP. These four groups of animals received similar behavioral tests as above on day 15, then were euthanized for tissue collection.

The pole test was conducted as previously described [32]. Briefly, a wooden pole (diameter 1 cm, height 50 cm) was placed vertically into the home cage, and the upper end of the pole was covered with a spherical protruding point with a diameter of 2 cm. The mouse was placed on the spherical protruding point with its head upward during the test. We recorded the respective time for the mouse to crawl from the spherical protruding point to the pole, from the top of the pole to the half of the pole, and from one-half of the pole to the bottom of the pole. We scored mouse performance as 3, 2, 1 or 0 if the animal finished the task at each stage within 3 s, 6 s, over 6 s, or fell from the pole, respectively.

The traction test was performed as previously described [33] to measure muscle strength and equilibrium. In brief, we placed the fore paws of the mouse on a horizontal wire (diameter 5 mm, length 100 cm) and scored mouse performance by counting the number of its hind paws to grasp the wire. A score of 3, 2, 1 or 0 was given to the animal if it grasped the wire with both hind paws, one hind paw, no hind paws, and fell from the wire, respectively.

We followed the procedure described in our previous study [28] to perform the rota-rod task. Five mice were positioned on the rota-rod containing 5 compartments, with one animal per compartment. Animals were trained to maintain themselves on the rod one day before the formal test. The rotation speed of the rod was set at 20 rpm and mice were tested for a total duration time of 180 s. After the rota-rod was switched on for 3 s, animals were timed until they fell off the rota-rod or were given a maximum cutoff time of 180 s if the animals did not fall off the rod during the test. Each animal had 3 consecutive trials per day, with the highest individual score being used in the analysis.

2.9. Histopathological staining

Mice were anesthetized with pentobarbital and were intracardially perfused with saline. The brains of mice were stripped and rinsed in cold PBS, followed by immediate dissection into two halves. One half was stored at −80 °C for biochemical assays. The other half of brain was fixed in 4% paraformaldehyde in PBS, which was then dehydrated successively with 15% and 30% sucrose solutions at 4 °C. The midbrain containing the SNc was sectioned at 10 μm thickness on a cryostat (RIWARD, Minux® FS800, Shenzheng, China). The immunohistochemical analysis was performed using the UltraSensitiveTMSP (Rabbit) IHC Kit (Fuzhou Maixin Biotech, KIT-9707) and DAB kit (Fuzhou Maixin Biotech, DAB-1031) according to the manufacturer's protocols. Primary rabbit anti-TH antibody (Millipore, AB152, 1:500) was used to assess the loss of dopamine neurons in the SNc. The stereological analysis of dopaminergic neurons was conducted as previously described [34] with minor modification. Briefly, at least five brain slices from each mouse were selected for analysis. The number of TH-positive cells in the SNc was counted by researchers blind to the treatment condition, and the average cell count per animal was used for statistical analysis.

2.10. Statistical analysis

All statistical analysis was performed by using GraphPad Prism v7.0. Student's *t*-test was used for quantifying difference between groups. Comparisons of relative protein levels of GSNOR, TH, CDK5, SQSTM1 and the LC3B-II:LC3B-I ratio from animals of multiple groups and cells with different treatments were conducted by one-way or two-way analysis of variance (ANOVA) with the Tukey post-hoc test. The traction test scores, pole test scores and rota rod task of WT and *Gsnor*$^{-/-}$ mice were assessed by using two-way ANOVA. All data are presented as mean ± standard deviation (SD). All tests were two-tailed. A *P*-value of <0.05 was considered to be statistically significant.

3. Results

3.1. MPTP induced CDK5-mediated autophagy and GSNOR upregulation

In the mouse PD model established by chronic MPTP treatment, we observed PD-like motor symptoms according to the behavioral tests and pathological defects as described in our previous study [28] and others [35–37]. Briefly, MPTP-treated mice exhibited a significantly decreased retention time on the rota-rod, lower scores in the traction test and pole test as compared to control mice treated with saline (Fig. S1A). Furthermore, MPTP injection drastically reduced the number of tyrosine hydroxylase (TH)-positive cells in the SNc (Figs. S1B and C) and decreased the protein level of TH in the striatal tissues of mice with MPTP treatment (Figs. S1D and E). We also detected the protein levels of GSNOR, CDK5, the indicator proteins of autophagy (sequestosome 1 (SQSTM1) and microtubule-associated protein 1 light chain 3 beta (LC3B)-I and LC3B-II [38] in the striatal tissues of mice with or without MPTP treatment. We observed an increased protein level of CDK5, together with an increased LC3B-II:LC3B-I ratio and a decreased level of SQSTM1 in mice with MPTP treatment (Figs. S1D and E). These results showed that MPTP induced CDK5-mediated autophagy in the striatal tissues of mice with MPTP treatment, as described in our previous study [28]. Interestingly, we found that the protein level of GSNOR was significantly increased in the striatal tissues of mice after MPTP treatment (Figs. S1D and E). Consistent with these observations in the mouse model, we were able to confirm the concomitant increase of CDK5-mediated autophagy and GSNOR expression induced by MPTP or MPP^+ in C6 (Figs. S2A and B) and PC12 cells (Figs. S2C and D). The results showed that CDK5-mediated autophagy is activated along with increased GSNOR expression in response to MPTP or MPP^+ treatment, and there is a potential link for GSNOR upregulation and CDK5-mediated autophagy in this process.

3.2. GSNOR knockout alleviated MPTP-induced behavioral dyskinesias, dopaminergic neuron loss

In order to determine the role of GSNOR in the pathogenesis of PD in the mouse model induced by MPTP, we conducted behavioral tests with wild type (WT) and *Gsnor* knockout ($Gsnor^{-/-}$) mice with chronic MPTP treatment. We observed that WT mice with MPTP treatment daily for 2 weeks had a significantly decreased retention time on the rota-rod, and decreased scores in the traction test and pole test as compared to the WT

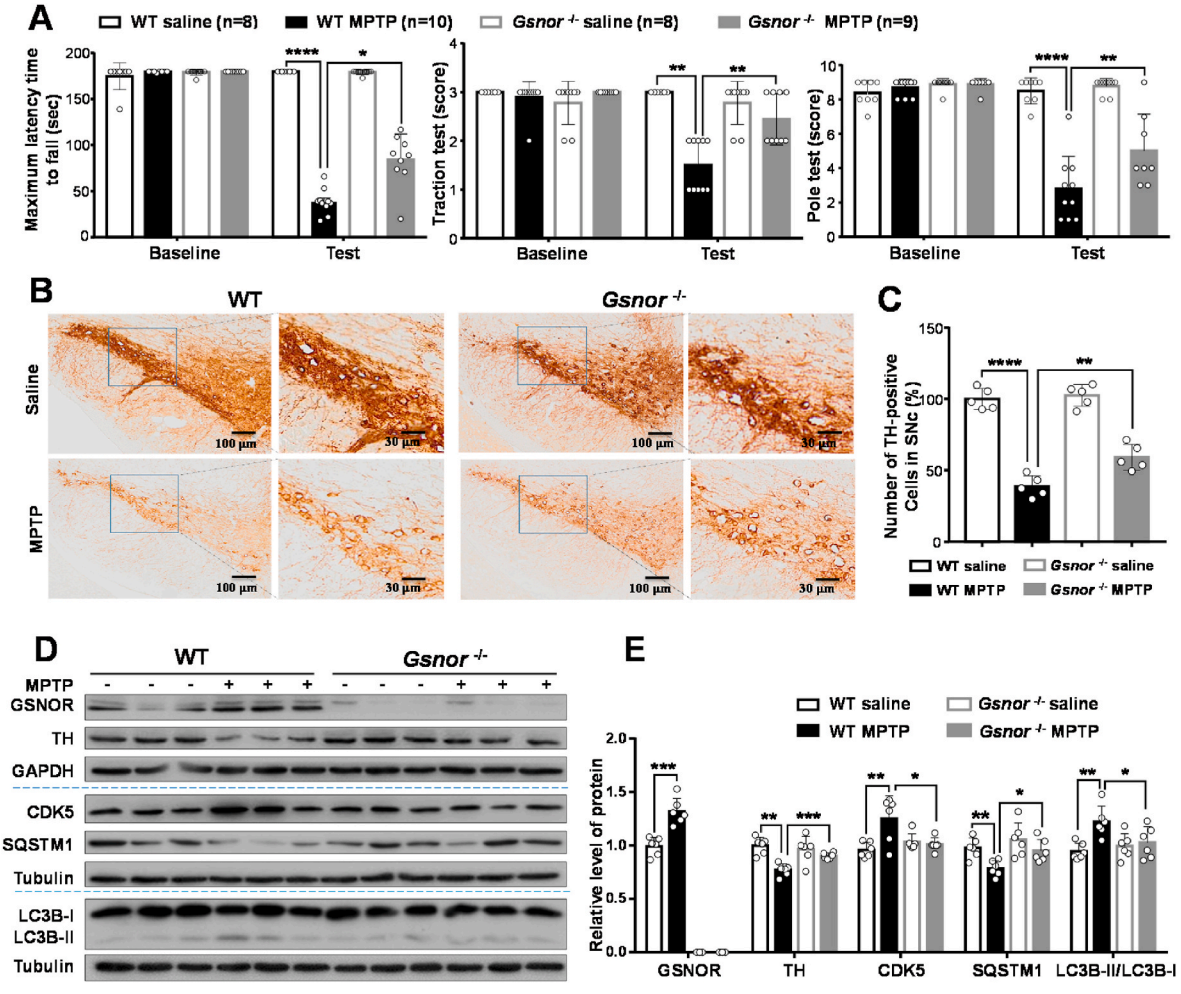

Fig. 1. GSNOR knockout alleviates MPTP-induced behavioral dyskinesias, dopaminergic neuron loss and CDK5-mediated autophagy.
(**A**) MPTP treatment in WT mice caused a significant decrease of performance as compared to WT mice without any treatment. This impairment induced by MPTP could be, in part, salvaged by *Gsnor* knockout ($Gsnor^{-/-}$). Animals were subjected to behavioral tests on Day 0 (Baseline), then received MPTP or saline daily for 2 weeks, and received behavioral tests on Day 15 (Test). (**B**) Representative TH immunoreactivity of the SNc region in WT and $Gsnor^{-/-}$ mice (n = 5 mice per group). (**C**) Quantification of the numbers of THpositive cells in (**B**). A single dot in the bar represents the average count for THpositive cells at least five slices of each animal. (**D–E**) Protein levels of GSNOR, TH, CDK5, SQSTM1, LC3B-II and LC3B-I in the striatal tissues from mice (n = 6 mice per group). GADPH or Tubulin was used as loading control. Data are normalized to the WT mice without MPTP treatment (WT saline group) and are presented as mean ± SD. *, $P < 0.05$; **, $P < 0.01$; ***, $P < 0.001$; ****, $P < 0.0001$; two-way ANOVA with the Tukey's post-hoc test.

saline group. Similarly, *Gsnor*$^{-/-}$ mice had a poorer performance after MPTP treatment as compared to *Gsnor*$^{-/-}$ mice with saline injection. However, *Gsnor*$^{-/-}$ mice had a significantly higher performance than WT mice on all three behavioral tests after MPTP treatment (Fig. 1A). These results indicated that knockout of *Gsnor* (partially) alleviated MPTP-induced behavioral dyskinesias in mice.

We further detected the number of dopaminergic neurons in the SNc of mice by using TH immunoreactivity after the behavioral tests. We found no difference in the number of TH-positive cells in *Gsnor*$^{-/-}$ mice as compared to WT mice in the saline group. MPTP treatment led to a significant reduction of THpositive cells in SNc of WT mice, but this damage induced by MPTP was significantly reduced in *Gsnor*$^{-/-}$ mice (Fig. 1B and C). Consistently, MPTP-treated WT mice had a significantly decreased level of TH protein in the striatal tissue as compared to the WT saline group, and knockout of *Gsnor* significantly attenuated the decreased TH level in the striatal tissue induced by MPTP treatment (Fig. 1D and E). These observations suggested an active role of GSNOR in the development of PD pathogenesis, and knockout of *Gsnor* was able to

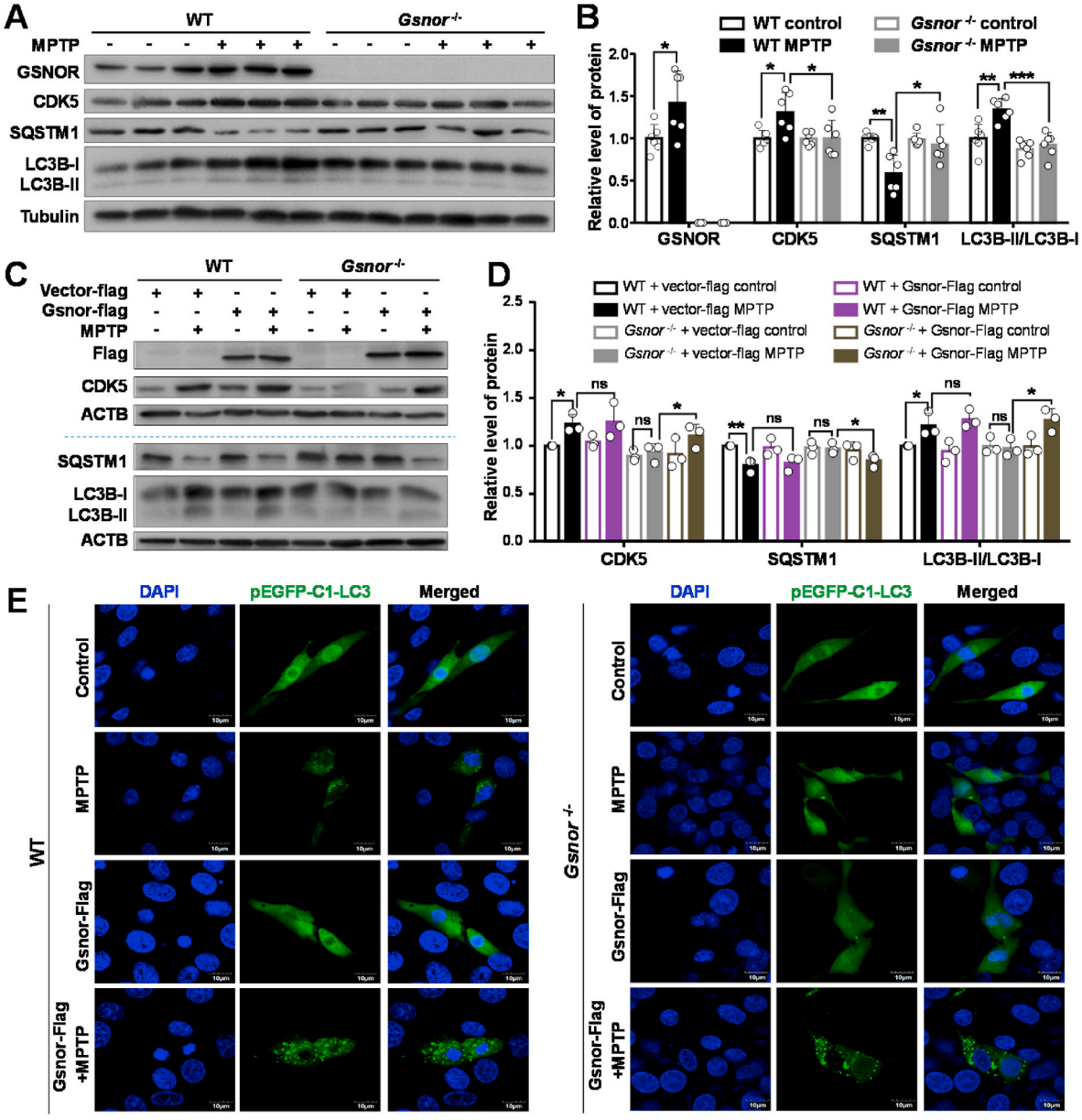

Fig. 2. GSNOR regulates CDK5-mediated autophagy in C6 cells.
(**A**) Protein levels of GSNOR, CDK5, SQSTM1, LC3B-II and LC3B-I in wild-type (WT) and GSNOR knockout (*Gsnor*$^{-/-}$) C6 cells with or without MPTP treatment. Tubulin was used as loading control. (**B**) Quantification of relative protein levels and LC3B-II:LC3B-I ratio in (**A**). (**C-D**) The CDK5-mediated autophagy induced by MPTP was blocked in C6 cells with GSNOR knockout, and GSNOR overexpression reversed this process. (**C**) Protein levels of CDK5, SQSTM1, LC3B-II and LC3B-I in WT and *Gsnor*$^{-/-}$ C6 cells overexpressing empty vector (Vector-flag) and GSNOR (Gsnor-Flag), with or without MPTP treatment. ACTB was used as loading control. (**D**) Quantification of relative protein levels of CDK5 and SQSTM1 and LC3B-II:LC3B-I ratio in (**C**). (**E**) Confocal microscopy assay for EGFP-LC3 puncta in WT and *Gsnor*$^{-/-}$ C6 cells with or without GSNOR overexpression and MPTP treatment. Cells were co-transfected with empty vector (Vector-flag) and N-terminally tagged pEGFP-C1-LC3 or GSNOR (Gsnor-Flag) and N-terminally tagged pEGFP-C1-LC3 for 24 h, then received MPTP (500 μM) treatment for another 24 h before the confocal microscopy assay. Shown results are representative of three independent experiments with similar results. Data are normalized to WT C6 cells without MPTP treatment (WT control) (**A**) and to WT C6 cells transfected with empty vector (Vector-flag) without MPTP treatment (WT + Vector-flag control) (**C**), respectively. Values are mean ± SD. ns, not significant; *, $P < 0.05$; **, $P < 0.01$; two-way ANOVA with the Tukey's post-hoc test was used in (**B**). One-way ANOVA with the Tukey's post-hoc test was used in (**D**).

alleviate MPTP-induced behavioral dyskinesias and dopaminergic neuron loss in mice.

3.3. GSNOR knockout alleviated MPTP-induced CDK5-mediated autophagy

We have previously shown that CDK5-mediated autophagy played an important role in the onset of PD [28]. To investigate whether GSNOR was involved in this process, we detected the protein levels of GSNOR, CDK5, SQSTM1, and LC3B-I and LC3B-II in the striatal tissues of mice with or without MPTP treatment. We observed increased protein levels of GSNOR and CDK5, together with an increased LC3B-II:LC3B-I ratio and a decreased level of SQSTM1 in mice with MPTP treatment. Moreover, the levels of the proteins were reversed by the knockout of the *Gsnor* gene (Fig. 1D and E). Consistent with the *in vivo* observations, knockout of GSNOR inhibited CDK5-mediated autophagy in C6 cells upon MPTP treatment (Fig. 2A and B) and PC12 cells upon MPP^+ treatment (Fig. S3). To further confirm GSNOR regulated MPTP-induced CDK5-mediated autophagy, we overexpressed GSNOR in C6 cells with GSNOR knockout. We observed an increased protein level of CDK5 and the LC3B-II:LC3B-I ratio, a decreased level of SQSTM1 (Fig. 2C and D), and an increase of EGFP-LC3 puncta (Fig. 2E) in WT C6 cells overexpressing vector-Flag or Gsnor-Flag after MPTP treatment. These changes were not observed in *Gsnor* knockout C6 cells overexpressing vector-Flag regardless of MPTP treatment (Fig. 2C–E). In contrast, overexpression of Gsnor-Flag in *Gsnor* knockout C6 cells rendered the cells more susceptible to MPTP-induced toxicity, and resembled those of the WT cells with MPTP treatment (Fig. 2C–E). Similarly, we were able to replicate the rescuing effect of GSNOR overexpression in PC12 cells with GSNOR knockout in response to MPP^+ treatment (Fig. S4). Taken together, these results suggested that GSNOR was involved in CDK5-mediated autophagy.

3.4. GSNOR knockout alleviated MPTP-induced CDK5 kinase activity and increased the S-nitrosation of CDK5

To explore whether GSNOR regulates CDK5, we measured the CDK5 kinase activity by using recombinant Histone H1 protein as the substrate, with a higher level of phosphorylation of Histone H1 corresponding to a higher CDK5 kinase activity [31]. We found that the protein level of phospho-Histone H1 was increased in the striatal tissues of WT mice injected with MPTP, suggesting an activation of CDK5 activity. Knockout of *Gsnor* could inhibit the protein level of phospho-Histone H1 regardless of MPTP treatment, which indicated that GSNOR deficiency inhibited CDK5 kinase activity in the striatal tissue of mice in response to MPTP treatment (Fig. 3A and B). We were able to replicate the observation that CDK5 kinase activity was inhibited by knockout of *Gsnor* in C6 cells (Fig. 3C and D). These results suggested that GSNOR negatively regulated CDK5 kinase activity.

As GSNOR is a key metabolic enzyme for *S*-nitrosation modification homeostasis [17], we hypothesized the GSNOR's inhibition effect on CDK5 kinase activity might be mediated by its *S*-nitrosation effect on CDK5. To determine whether GSNOR regulates the *S*-nitrosation of CDK5, we determined whether CDK5 can be *S*-nitrosated by the GSNO, an nitric oxide donor for inducing protein *S*-nitrosation within a very short time (5–15 min) [39,40]. Glutathione (GSH), a compound that can induce the denitrosation of protein [39], was used as another control. Cell lysates of C6 cells were incubated with GSNO (500 μM) or GSH (500 μM) for 30 min, then were subjected to biotin switch assay in the presence or absence of ascorbate. Consistent with previous studies [39], we found that in the presence of ascorbate, CDK5 was readily *S*-nitrosated after GSNO treatment compared to that of without GSNO treatment (Fig. S5A). In contrast, *S*-nitrosated CDK5 was not detected in the presence of GSH and absence of ascorbate (Fig. S5A). These results suggested that CDK5 can be *S*-nitrosated *in vitro* [39], and our experiment system was workable. Next, we performed the biotin switch assay to detect potential effect of GSNOR on *S*-nitrosation of CDK5 following reported method [29,30]. In WT mice, the degree of CDK5 *S*-nitrosation was significantly reduced by MPTP (Fig. 3E and F), consistent with the observed higher level of CDK5 kinase activity (Fig. 3A and B). In $Gsnor^{-/-}$ mice with or without MPTP treatment, we observed a high level of CDK5 *S*-nitrosation in striatal tissue (Fig. 3E and F), consistent with the above-mentioned blockage effect on CDK5-mediated effect by knockout of *Gsnor* in mice. The observation seen in mouse striatal tissue

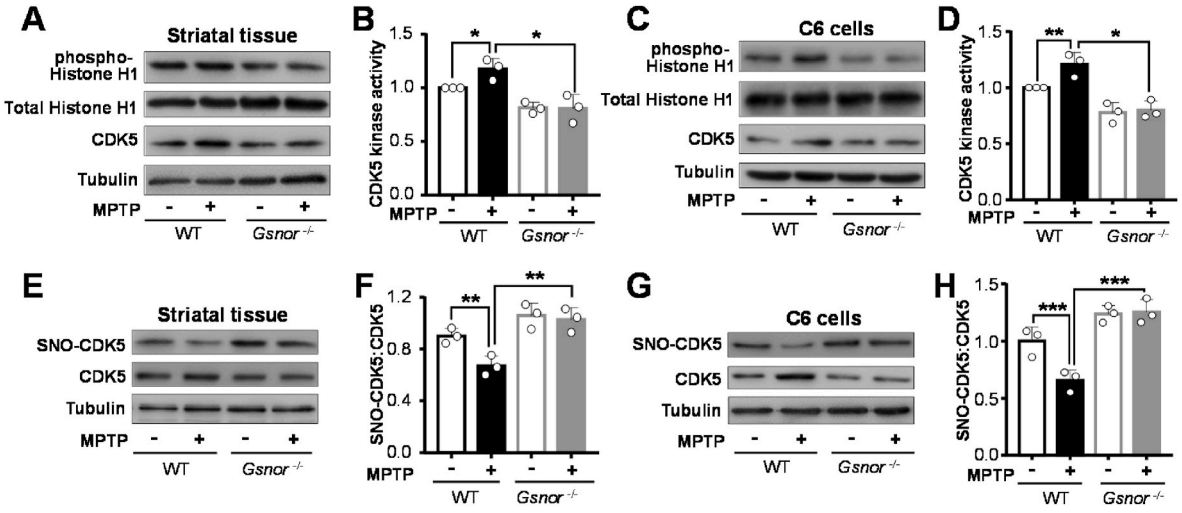

Fig. 3. GSNOR knockout alleviates MPTP-induced CDK5 kinase activity and increases *S*-nitrosation of CDK5. (**A**) CDK5 protein levels in the striatal tissues of WT and $Gsnor^{-/-}$ with or without MPTP treatment and its capability for phosphorylation of substrate Histone H1 (n = 3 mice per group). (**B**) Quantification of CDK5 kinase activity as measured by phospho-histone H1:total Histone H1 ratio in (**A**). (**C**) CDK5 protein levels in WT and GSNOR knockout ($Gsnor^{-/-}$) C6 cells with or without MPTP treatment and its capability for phosphorylation of substrate Histone H1. (**D**) Quantification of CDK5 kinase activity as measured by phospho-histone H1:total Histone H1 ratio in (**C**). (**E**) Levels of *S*-nitrosated CDK5 and total CDK5 in the striatal tissues of WT and $Gsnor^{-/-}$ with or without MPTP treatment (n = 3 mice per group). (**F**) Quantification of CDK5 *S*-nitrosation level in (**E**). (**G**) Levels of *S*-nitrosated CDK5 and total CDK5 in WT and GSNOR knockout ($Gsnor^{-/-}$) C6 cells with or without MPTP treatment. (**H**) Quantification of CDK5 *S*-nitrosation level in (**G**). Shown data for C6 cells in (**C**) and (**G**) are representative of three independent experiments with similar results. Data are normalized to the WT mice (**A**) and C6 cells (**C**) without MPTP treatment (WT control) and values are mean ± SD. *, $P < 0.05$; **, $P < 0.01$; ***, $P < 0.001$; two-way ANOVA with the Tukey's post-hoc test.

was replicated by using the C6 cells, in which the degree of CDK5 *S*-nitrosation was significantly increased in *Gsnor* knockout C6 cells (Fig. 3G and H). These results suggested that GSNOR regulated the degree of CDK5 *S*-nitrosation in mice and cells.

3.5. *S*-nitrosation of CDK5 at Cys83 inhibited CDK5 kinase activity and CDK5-mediated autophagy

To determine the site(s) of *S*-nitrosation on CDK5, we focused on the cysteine (Cys) residues of CDK5, which constitute potential sites for *S*-nitrosation. The CDK5 protein has eight cysteine residues and we created mutants with the respective cysteine residue being mutated to serine (Ser) (Fig. 4A). C6 cells were transfected with expression vectors of wild-type CDK5 with Myc-tag (Myc-CDK5-WT), CDK5 mutants (p.C53S, p.C83S, p.C94S, p.C117S, p.C157S, p.C190S, p.C269S and p.C290S), and empty vector (vector-Myc), respectively. Cell lysates were then incubated with GSNO for 30 min before the biotin switch assay. GSNO treatment significantly increased the *S*-nitrosation of Myc-CDK5-WT and five cysteine mutants of CDK5 (p.C53S, p.C94S, p.C157S, p.C269S and p.C290S). Mutations at Cys83, Cys117 and Cys190, partially abolished the *S*-nitrosation of CDK5, suggested that these three cysteine residues were major sites of *S*-nitrosation of CDK5 (Fig. 4B and C).

Next, we explored whether the *S*-nitrosation of CDK5 affected its kinase activity. C6 cells were transfected with expression vector for Myc-CDK5-WT or each cysteine mutant (p.C83S, p.C117S and p.C190S) that affected the *S*-nitrosation of CDK5. We found that mutant CDK5 p.C83S increased the level of phospho-Histone H1, suggesting an increased kinase activity of this mutant (Fig. 4D and E). This result was consistent with a previous observation that used recombinant proteins of CDK5 and mutant CDK5 p.C83S to show an increased kinase activity of the mutant [39]. However, mutants p.C117S and p.C190S did not affect kinase activity of CDK5, as cells overexpressing these mutants presented a similar level of phospho-Histone H1 with those overexpressing Myc-CDK5-WT (Fig. 4D and E). These results showed that the 83rd Cys of CDK5 is the major site regulating CDK5 kinase activity through *S*-nitrosation, which was also reported in previous studies [39,41]. So as to find if *S*-nitrosation of CDK5 affected autophagy by regulating CDK5 kinase activity, we transfected C6 cells with Myc-CDK5-WT and CDK5

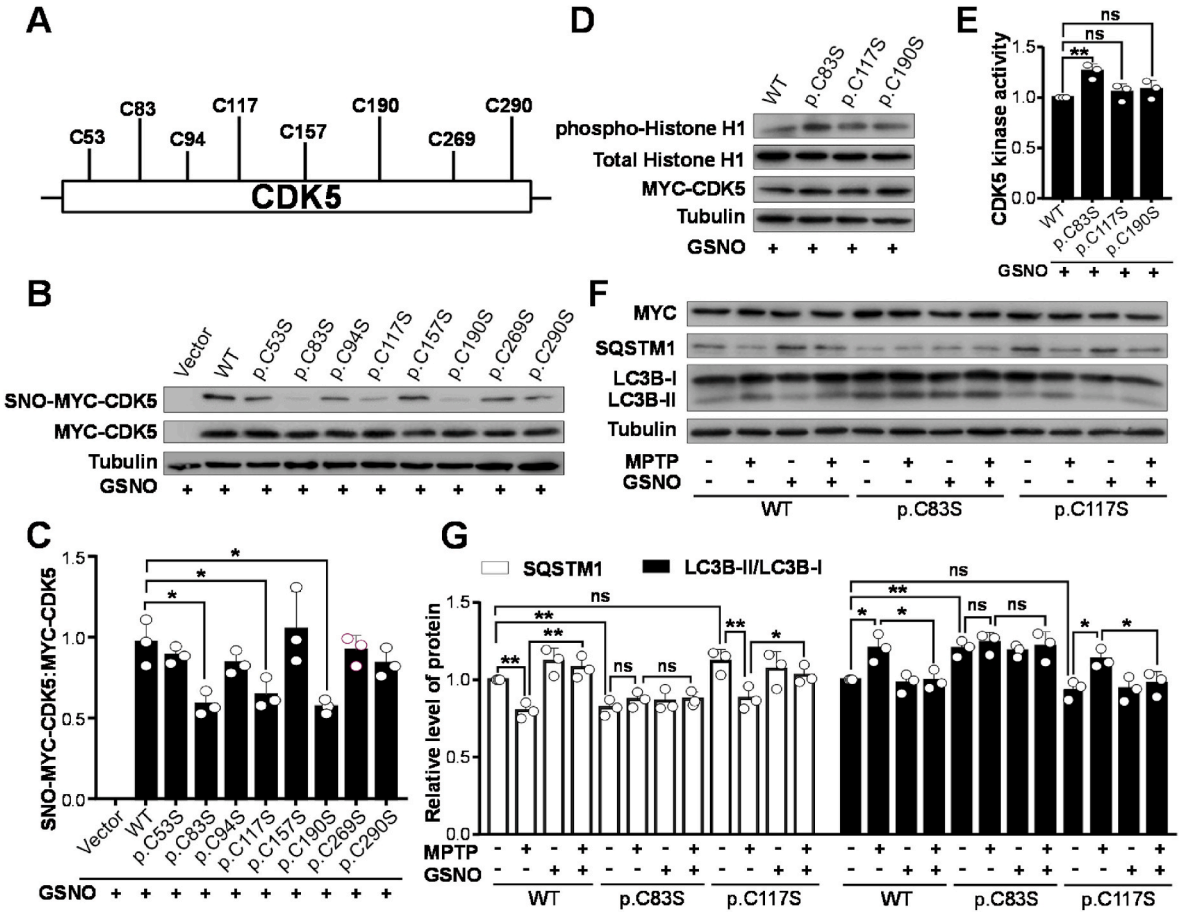

Fig. 4. *S*-nitrosation of CDK5 at Cys83 inhibits CDK5 kinase activity and autophagy. (**A**) Schematic diagram showing all eight potential *S*-nitrosation sites of CDK5. (**B**) Levels of *S*-nitrosated exogenous CDK5 and total exogenous CDK5 in C6 cells after GSNO treatment. Cells were transfected with expression vectors of wild type CDK5 (WT), cysteine mutants of CDK5 (p.C53S, p.C83S, p.C94S, p.C117S, p.C157S, p.C190S, p.C269S and p.C290S) and empty vector (Vector) for 48 h. Cell lysates were incubated with GSNO (500 μM) for 30 min before the biotin switch assay. (**C**) Quantification of exogenous CDK5 *S*-nitrosation level in C6 cells based on three independent experiments with similar results. Data are normalized to the cells with transfection of wild type CDK5 (WT), and bars refer to mean ± SD. (**D**) The phosphorylation capability of wild type (WT) CDK5 and its cysteine mutants (p.C83S, p.C117S and p.C190S) for substrate Histone H1. C6 cells were transfected with expression vector of wild type CDK5 (WT) or CDK5 cysteine mutants (p.C83S, p.C117S or p.C190S) for 24 h, then received a pretreatment with GSNO (500 μM) for another 24 h. (**E**) Quantification of CDK5 kinase activity as measured by phospho-histone H1:total Histone H1 ratio in (**D**). (**F**) Different effects of overexpression of wild type CDK5 (WT) and its cysteine mutants (p.C83S and p.C117S) on CDK5-mediated autophagy in C6 cells. C6 cells were transfected with expression vector of wild type CDK5 (WT) or CDK5 cysteine mutants (p.C83S, p.C117S) for 24 h, then received a pretreatment with GSNO (500 μM) for 30 min before the treatment with or without MPTP (500 μM). Tubulin was used as loading control. (**G**) Quantification of protein level of SQSTM1 and LC3B-II:LC3B-I ratio in (**F**). Shown results are representative of three independent experiments with similar results. Data are normalized to WT C6 cells transfected with expression vector of wild type CDK5 (WT) without GSNO and MPTP treatment. Values are present as mean ± SD. ns, not significant; *, $P < 0.05$; **, $P < 0.01$; one-way ANOVA with the Tukey's post-hoc test.

mutants (p.C83S, p.C117S and p.C190S), respectively. We found that MPTP treatment increased the LC3B-II:LC3B-I ratio and decreased SQSTM1 level in cells overexpressing Myc-CDK5-WT, mutants p.C117S (Fig. 4F and G) and p.C190S (Fig. S6), and this effect could be reversed by a pretreatment with GSNO (Fig. 4F and G). These results demonstrated that the two sites of CDK5 (Cys117 and Cys190) did not affect MPTP-induced autophagy, consistent with the above observation that these two mutants had no effect on CDK5 kinase activity (Fig. 4D and E). Concordantly, mutant CDK5 p.C83S increased the LC3B-II:LC3B-I ratio and decreased SQSTM1 level in transfected cells with or without MPTP treatment compare to those transfected with Myc-CDK5-WT or mutants p.C117S (Fig. 4F and G) and p.C190S (Fig. S6). These results demonstrated that *S*-nitrosation of CDK5 at Cys83 inhibited MPTP-induced autophagy by inhibiting CDK5 kinase activity.

3.6. Inhibition of GSNOR by N6022 alleviated MPTP-induced neurotoxicity

N6022, which is a safe, specific and reversible inhibitor of GSNOR [42,43], has been used in the studies of GSNOR-related diseases with few side effects [42,44,45]. Meanwhile, peripheral injection of N6022 could reduce infarct volume in both striatal and cortical regions of cerebral ischemia and reperfusion mice [46], suggesting that this inhibitor can cross the blood-brain barrier. We therefore determined whether N6022 would have a beneficial effect on MPTP-induced neurotoxicity. The mice given N6022 as a pretreatment before MPTP injection (N6022+MPTP group) showed a reduced degree of behavioral dyskinesias as compared to the mice without N6022 pretreatment but just MPTP treatment (Vehicle + MPTP group) (Fig. 5A). Pretreatment with N6022 also rescued MPTP-induced pathological changes, including decreased level of TH protein, and inhibited CDK5-mediated autophagy as compare to the Vehicle + MPTP group (Fig. 5B and C). Similarly, compared to mice with MPTP treatment alone, N6022 pretreatment inhibited the CDK5 kinase activity (Fig. 5D and E) and increased the *S*-nitrosation of CDK5 in the striatal tissues from the mice with or without MPTP treatment (Fig. 5F and G). These results indicated that inhibition of GSNOR may be an effective way to prevent PD at the early stage, and further confirmed that GSNOR is a critical regulator in the pathogenesis of mouse PD model.

4. Discussion

PD is a neurodegenerative disease characterized by the accumulation of Lewy body aggregates and dopaminergic neuron death in the SNc region. The development of PD is affected by protein misfolding, aggregation, and abnormal expression [47], which are regulated, in part, by protein modifications [9]. Autophagy is a very important process for the clearance of misfolded proteins [38] such as α-synuclein oligomer [48,49]. As a cellular denitrosase, GSNOR reduces cellular levels of *S*-nitrosation of protein and GSNO [17]. In the present study, we determined the role of GSNOR, *S*-nitrosation of CDK5 and CDK5-mediated autophagy in the development of PD using both a

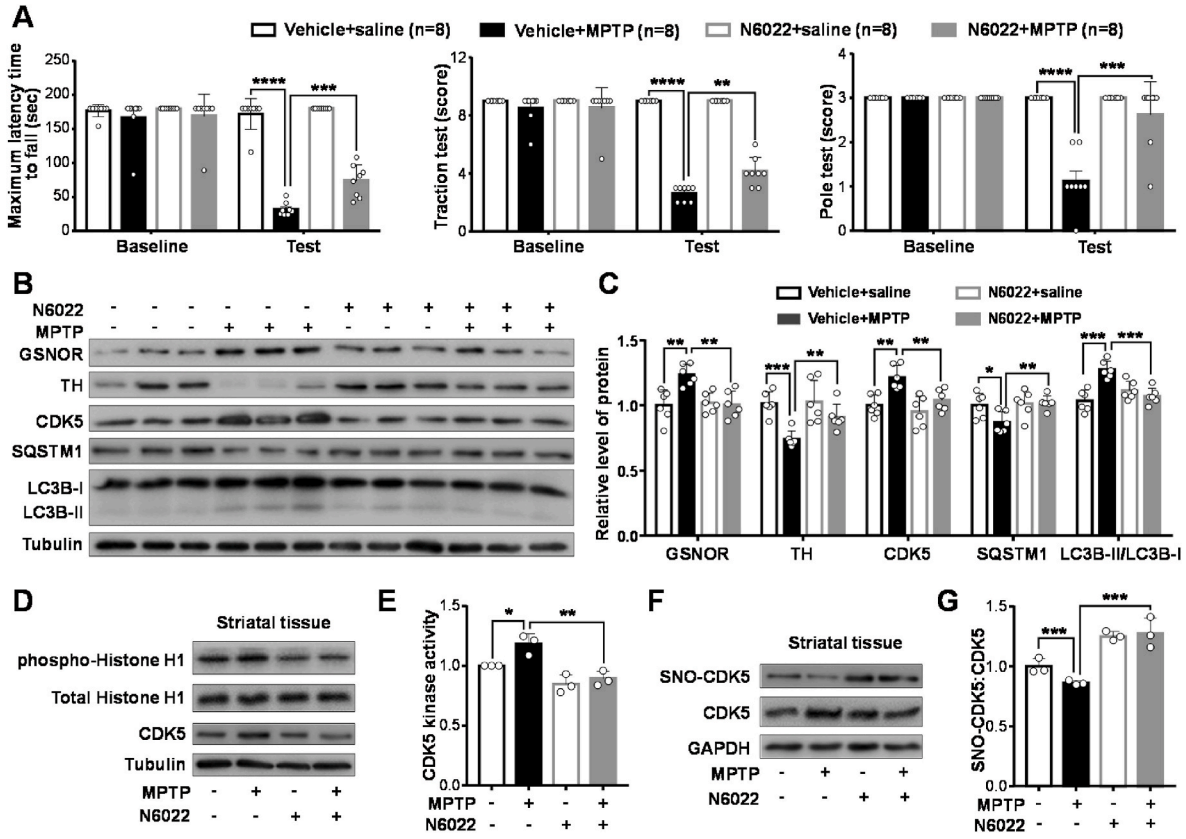

Fig. 5. Inhibition of GSNOR alleviates MPTP-induced neurotoxicity.
(**A**) Pretreatment with N6022 before MPTP treatment in WT mice has a beneficial effect on MPTP-induced behavioral dyskinesias. Animals were subjected to the behavioral tests on Day 0 (Baseline), then received N6022 or vehicle 30 min before MPTP or saline daily for 2 weeks, and had the behavioral tests on Day 15 (Test). (**B-C**) Protein levels of GSNOR, TH, CDK5, SQSTM1, LC3B-II and LC3B-I in striatal tissues from mice in (**A**) (n = 6 mice per group). Tubulin was used as loading control. (**D**) CDK5 protein levels in the striatal tissues of mice in (**A**) and its capability for phosphorylation of substrate Histone H1. (**E**) Quantification of CDK5 kinase activity (n = 3 mice per group) as measured by phospho-histone H1:total Histone H1 ratio in (**D**). (**F**) Levels of *S*-nitrosated CDK5 and total CDK5 in the striatal tissues of mice with or without treatment of N6022 and/or MPTP. Each group has 3 mice. (**G**) Quantification of CDK5 *S*-nitrosation level (n = 3 mice per group) in (**F**). Data are normalized to the WT mice without N6022 and MPTP treatment (Vechicle + saline). Values are presented as mean ± SD. *, $P < 0.05$; **, $P < 0.01$; ***, $P < 0.001$; ****, $P < 0.0001$; two-way ANOVA with the Tukey's post-hoc test.

MPTP-induced mouse model and cellular models. We found that the protein level of GSNOR and CDK5-mediated autophagy were increased in the MPTP-induce mouse PD model. Genetic deletion of GSNOR attenuated CDK5-mediated autophagy, reduced MPTP-induced behavioral dyskinesias and prevented dopaminergic neuron loss. The beneficial effects of GSNOR deficiency were associated with the preservation of *S*-nitrosation of CDK5, which inhibited its kinase activity and further inhibited MPTP-induced autophagy (Fig. 6). The beneficial effects offered by GSNOR deficiency could be duplicated by using a GSNOR inhibitor N6022 before MPTP treatment. All these results suggested that GSNOR plays a key role in MPTP-mediated neurotoxicity via *S*-nitrosation of CDK5 and inhibition of CDK5-mediated autophagy.

The *S*-nitrosation of proteins plays a pivotal role in the molecular switches triggering signaling cascades [50]. A reasonable level of *S*-nitrosation is very important for maintaining normal physiological activities [51]. GSNO serves as the main reservoir of nitric oxide that governs *S*-nitrosation of proteins in organisms. Abnormal metabolism of GSNO mediated by GSNOR may destroy homeostasis of *S*-nitrosation of proteins and lead to serious consequences for cellular function and survival [17]. Previous studies reported an aberrant increase of GSNOR protein and enzymatic activity in a variety of diseases including asthma [52], cognitive impairment [24], stroke [46], myocardial infarction [53], and cerebral malaria [54]. Knockdown of GSNOR was found to improve MPP^+-induced toxicity in cellular models [25]. However, there were some studies showing that GSNOR knockout promoted the *S*-nitrosation of parkin and led to mitophagy defects [55,56], which caused a detrimental effect, instead of beneficial effect on the disease progression. These studies showed that GSNOR may play different roles in different pathological conditions, dependent on the preconditions and the stages of diseases. In the present study, we found that both genetic deletion of *Gsnor* and pharmacological inhibition of GSNOR by using N6022, contributed to the maintenance of *S*-nitrosation of CDK5 in mice after MPTP treatment and inhibited MPTP-induced autophagy and neurotoxicity. This result provided direct evidence that GSNOR-mediated denitrosation of proteins has an active involvement in the development of PD. We previously found that melatonin could reduce the MPTP-induced CDK5 protein expression [28], similar to the effect of GSNOR knockout in cells with MPTP treatment as observed here. Concordantly, melatonin pretreatment could reverse the MPTP-induced reduction of CDK5 *S*-nitrosation (Fig. S5B). This result further enhanced the conclusion for a key role of the GSNOR-medicated denitrosation in MPTP neurotoxicity.

Autophagy is an essential degradation process to maintain cellular homeostasis and promote cell survival [57]. Emerging evidence has suggested that autophagy dysfunction is involved in the pathogenesis of PD [58,59], and autophagy plays an important role in the degradation of misfolded proteins in PD such as α-synuclein oligomer [49]. However, in certain conditions, autophagy might act as a double-edged sword in the development of PD [57,60]. *S*-nitrosation of proteins, such as PTEN [61], Bcl-2 [62] and JNK1 and IKKβ [63], was involved in autophagy. In our previous studies [28,64], we found that the *S*-nitrosation of ATG4B directly regulated autophagy in response to high glucose [64], and CDK5-mediated autophagy played a key role in the PD-like symptom induced by MPTP [28]. The present study uncovered the potential mechanism for regulatory effects of GSNOR on CDK5-mediated autophagy by targeting the *S*-nitrosation of CDK5. As a cell-cycle dependent

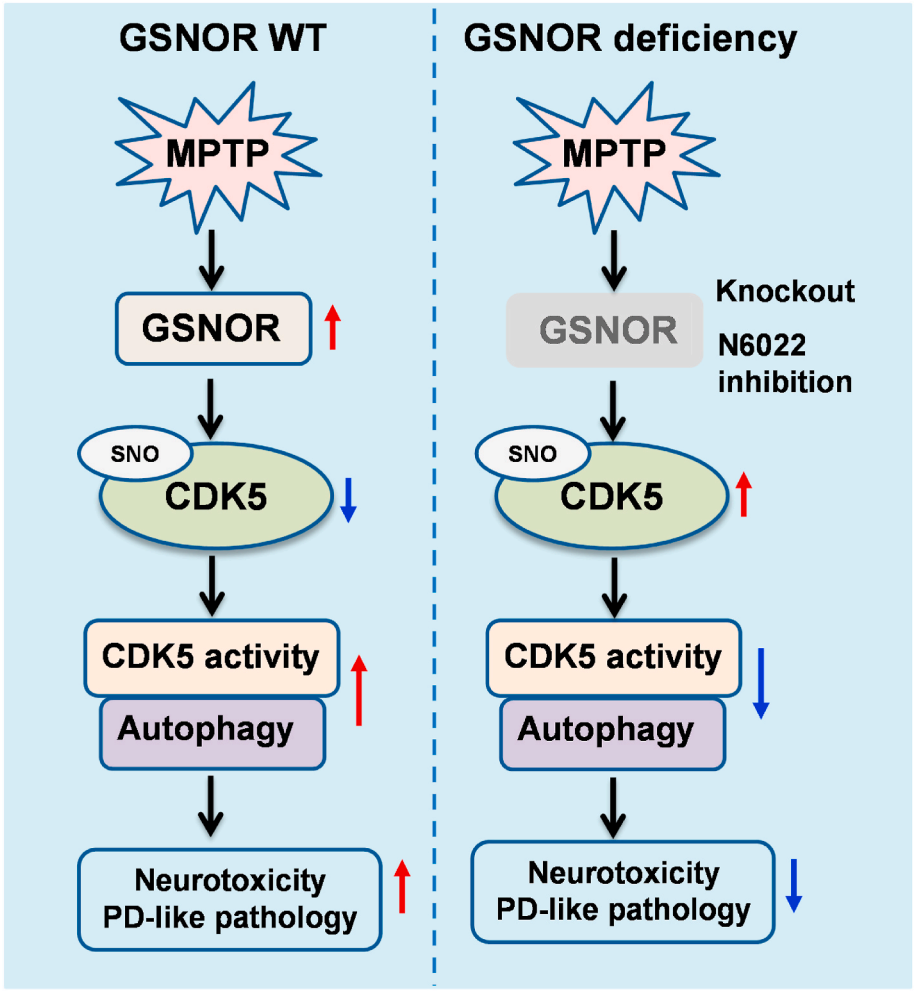

Fig. 6. The role of GSNOR in MPTP-induced Parkinsonism. The protein level of GSNOR was upregulated in MPTP-induced PD mouse model. Knockout of the *Gsnor* gene or inhibition of GSNOR by using specific inhibitor N6022 had an alleviating effect on MPTP-induced neurotoxicity by increasing *S*-nitrosation (SNO) of CDK5, which led to a reduced CDK5 kinase activity and CDK5-mediated autophagy. The colored up and down arrows refer to upregulation and downregulation of certain target, respectively.

kinase, CDK5 is closely involved in the pathogenesis of PD and other neurodegenerative diseases by regulating the phosphorylation of its substrates [60,65–68], and its kinase activity was activated in MPTP-induced PD models [69]. Protein post-translational modifications have been reported to regulate CDK5 kinase activity. For example, phosphorylation of CDK5 at Tyrosine15 [70] and at Serine159 [71] is essential for catalytic activity of CDK5, and *S*-nitrosation of CDK5 at Cys83 site is closely involved in its kinase activity [39,41]. As had been pointed out in a previous report [39], Cys83 residue is located in the ATP-binding pocket of CDK5, *S*-nitrosation of the 83rd Cys may perturbs the access of the kinase to ATP, and leads to suppression of its activation. In our study, we confirmed that *S*-nitrosation of CDK5 at the Cys83 site, but not at the other cysteines of CDK5, inhibited its kinase activity [39] and attenuated MPTP-induced autophagy. These findings revealed a previously unknown mechanism that GSNOR affects the kinase activity of CDK5 by regulating the *S*-nitrosation of CDK5, finally affects MPTP-induced autophagy and neurotoxicity mediated by CDK5.

There are three limitations in this study. First, we found that GSNOR regulated the MPTP-induced neurotoxicity and CDK5-mediated autophagy by *S*-nitrosation of CDK5 at Cys83; and it is appropriate to create a $CDK5^{C83S}$ knock-in mouse model to further validate this observation. Second, GSNOR knockout might have a widespread effect on *S*-nitrosation of proteins. According to a previous study [55], GSNOR deficiency can induce *S*-nitrosation of numerous protein targets, it is plausible that *S*-nitrosation of other targets, besides CDK5 as shown here, would provide a protective role by unknown pathways. Moreover, we did not analyze how CDK5 was *S*-nitrosated and how the balance between *S*-nitrosation and denitrosation of CDK5 was maintained *in vivo* in the physiological and pathological conditions. Future fine-grained proteomics assays based mass spectrometry may be helpful in answering this question. Third, although we showed that a pretreatment with N6022 had a protective effect on MPTP-induced neurotoxicity, we did not test whether N6022 treatment had a clinical effectiveness in curing PD, which would be rewarding to be tested.

5. Conclusions

In summary, we discovered a link between GSNOR, *S*-nitrosation of CDK5, and CDK5-mediated autophagy in PD. Knockout or chemical inhibition of GSNOR regulates CDK5-mediated autophagy by affecting the *S*-nitrosation of CDK5 and its kinase activity. Our work also indicated that inhibition of GSNOR, maintenance of *S*-nitrosation in CDK5, or inhibition of CDK5-mediated autophagy, may represent potential ways to alleviate PD.

Author contributions

Yong-Gang Yao, Lijin Jiao, and Ling-Yan Su conceived and designed the experiments. Lijin Jiao, Ling-Yan Su, Qianjin Liu, Rongcan Luo, Xinhua Qiao, Ting Xie, and Lu-Xiu Yang performed the experiments and analyzed the data. Chang Chen contributed to experimental design, interpretation of the results. Lijin Jiao and Yong-Gang Yao wrote the manuscript. All authors reviewed the content and approved the final version for publication.

Declaration of competing interest

There were no potential conflicts of interest to be disclosed.

Acknowledgments

We are grateful to Dr. Ian Logan for helpful comments and language editing of the manuscript and Dr. Tianle Gu for technical assistance. This study was supported by National Natural Science Foundation of China (31730037 to Y.G.Y., 91849203 to C.C. and 31900695 to L.Y.S.), the Applied Basic Research Foundation of Yunnan Province (202001AT070103 and 202201AW070017 to L.Y.S), Strategic Priority Research Program (B) of CAS (XDB02020003 to Y.G.Y. and XDB39000000 to C.C.) and Project for the Bureau of Frontier Sciences and Education, CAS (QYZDJ-SSW-SMC005 to Y.G.Y.).

Appendix A. Supplementary data

Supplementary data to this article can be found online at https://doi.org/10.1016/j.freeradbiomed.2022.07.016.

References

[1] A. Samii, J.G. Nutt, B.R. Ransom, Parkinson's disease, Lancet 363 (2004) 1783–1793.
[2] L.V. Kalia, A.E. Lang, Parkinson's disease, Lancet 386 (2015) 896–912.
[3] D.A. Kia, D. Zhang, S. Guelfi, C. Manzoni, L. Hubbard, R.H. Reynolds, J. Botia, M. Ryten, R. Ferrari, P.A. Lewis, N. Williams, D. Trabzuni, J. Hardy, N.W. Wood, Identification of candidate Parkinson disease genes by integrating genome-wide association study, expression, and epigenetic data sets, JAMA Neurol. 78 (2021) 464–472.
[4] C. Blauwendraat, M.A. Nalls, A.B. Singleton, The genetic architecture of Parkinson's disease, Lancet Neurol. 19 (2020) 170–178.
[5] P. Gonzalez-Rodriguez, E. Zampese, K.A. Stout, J.N. Guzman, E. Ilijic, B. Yang, T. Tkatch, M.A. Stavarache, D.L. Wokosin, L. Gao, M.G. Kaplitt, J. Lopez-Barneo, P. T. Schumacker, D.J. Surmeier, Disruption of mitochondrial complex I induces progressive parkinsonism, Nature 599 (2021) 650–656.
[6] R. Tufi, S. Gandhi, I.P. de Castro, S. Lehmann, P.R. Angelova, D. Dinsdale, E. Deas, H. Plun-Favreau, P. Nicotera, A.Y. Abramov, A.E. Willis, G.R. Mallucci, S.H. Loh, L. M. Martins, Enhancing nucleotide metabolism protects against mitochondrial dysfunction and neurodegeneration in a PINK1 model of Parkinson's disease, Nat. Cell Biol. 16 (2014) 157–166.
[7] N. Panicker, P. Ge, V.L. Dawson, T.M. Dawson, The cell biology of Parkinson's disease, J. Cell Biol. 220 (2021).
[8] F.M. de Araujo, L. Cuenca-Bermejo, E. Fernandez-Villalba, S.L. Costa, V.D.A. Silva, M.T. Herrero, Role of microgliosis and NLRP3 inflammasome in Parkinson's disease pathogenesis and therapy, Cell. Mol. Neurobiol. 42 (2022) 1283–1300.
[9] T. Nakamura, C.K. Oh, X. Zhang, S.A. Lipton, Protein S-nitrosylation and oxidation contribute to protein misfolding in neurodegeneration, Free Radic. Biol. Med. 172 (2021) 562–577.
[10] C.T. Stomberski, D.T. Hess, J.S. Stamler, Protein S-nitrosylation: determinants of specificity and enzymatic regulation of S-nitrosothiol-based signaling, Antioxidants Redox Signal. 30 (2019) 1331–1351.
[11] T. Nakamura, S. Tu, M.W. Akhtar, C.R. Sunico, S. Okamoto, S.A. Lipton, Aberrant protein s-nitrosylation in neurodegenerative diseases, Neuron 78 (2013) 596–614.
[12] K.K. Chung, B. Thomas, X. Li, O. Pletnikova, J.C. Troncoso, L. Marsh, V.L. Dawson, T.M. Dawson, S-nitrosylation of parkin regulates ubiquitination and compromises parkin's protective function, Science 304 (2004) 1328–1331.
[13] J. Fang, T. Nakamura, D.H. Cho, Z. Gu, S.A. Lipton, S-nitrosylation of peroxiredoxin 2 promotes oxidative stress-induced neuronal cell death in Parkinson's disease, Proc. Natl. Acad. Sci. U. S. A. 104 (2007) 18742–18747.
[14] A.H. Tsang, Y.I. Lee, H.S. Ko, J.M. Savitt, O. Pletnikova, J.C. Troncoso, V. L. Dawson, T.M. Dawson, K.K. Chung, S-nitrosylation of XIAP compromises neuronal survival in Parkinson's disease, Proc. Natl. Acad. Sci. U. S. A. 106 (2009) 4900–4905.
[15] M.S. Choi, T. Nakamura, S.J. Cho, X. Han, E.A. Holland, J. Qu, G.A. Petsko, J. R. Yates 3rd, R.C. Liddington, S.A. Lipton, Transnitrosylation from DJ-1 to PTEN attenuates neuronal cell death in Parkinson's disease models, J. Neurosci. 34 (2014) 15123–15131.
[16] C.K. Oh, A. Sultan, J. Platzer, N. Dolatabadi, F. Soldner, D.B. McClatchy, J. K. Diedrich, J.R. Yates 3rd, R. Ambasudhan, T. Nakamura, R. Jaenisch, S.A. Lipton, S-nitrosylation of PINK1 attenuates PINK1/Parkin-dependent mitophagy in hiPSC-based Parkinson's disease models, Cell Rep. 21 (2017) 2171–2182.
[17] L. Liu, A. Hausladen, M. Zeng, L. Que, J. Heitman, J.S. Stamler, A metabolic enzyme for S-nitrosothiol conserved from bacteria to humans, Nature 410 (2001) 490–494.
[18] H. Wu, I. Romieu, J.J. Sienra-Monge, B. Estela Del Rio-Navarro, D.M. Anderson, C. A. Jenchura, H. Li, M. Ramirez-Aguilar, I. Del Carmen Lara-Sanchez, S.J. London, Genetic variation in S-nitrosoglutathione reductase (GSNOR) and childhood asthma, J. Allergy Clin. Immunol. 120 (2007) 322–328.
[19] F. Beigi, D.R. Gonzalez, K.M. Minhas, Q.A. Sun, M.W. Foster, S.A. Khan, A. V. Treuer, R.A. Dulce, R.W. Harrison, R.M. Saraiva, C. Premer, I.H. Schulman, J. S. Stamler, J.M. Hare, Dynamic denitrosylation via S-nitrosoglutathione reductase regulates cardiovascular function, Proc. Natl. Acad. Sci. U. S. A. 109 (2012) 4314–4319.
[20] C.H. Tang, W. Wei, M.A. Hanes, L. Liu, Hepatocarcinogenesis driven by GSNOR deficiency is prevented by iNOS inhibition, Cancer Res. 73 (2013) 2897–2904.
[21] C. Montagna, G. Di Giacomo, S. Rizza, S. Cardaci, E. Ferraro, P. Grumati, D. De Zio, E. Maiani, C. Muscoli, F. Lauro, S. Ilari, S. Bernardini, S. Cannata, C. Gargioli, M. R. Ciriolo, F. Cecconi, P. Bonaldo, G. Filomeni, S-nitrosoglutathione reductase deficiency-induced S-nitrosylation results in neuromuscular dysfunction, Antioxidants Redox Signal. 21 (2014) 570–587.

[22] J. Li, Y. Zhang, Y. Zhang, S. Lu, Y. Miao, J. Yang, S. Huang, X. Ma, L. Han, J. Deng, F. Fan, B. Liu, Y. Huo, Q. Xu, C. Chen, X. Wang, J. Feng, GSNOR modulates hyperhomocysteinemia-induced T cell activation and atherosclerosis by switching Akt S-nitrosylation to phosphorylation, Redox Biol. 17 (2018) 386–399.
[23] Q. Liu, T. Gu, L.Y. Su, L. Jiao, X. Qiao, M. Xu, T. Xie, L.X. Yang, D. Yu, L. Xu, C. Chen, Y.G. Yao, GSNOR facilitates antiviral innate immunity by restricting TBK1 cysteine S-nitrosation, Redox Biol. 47 (2021), 102172.
[24] Y. Zhang, K. Wu, W. Su, D.F. Zhang, P. Wang, X. Qiao, Q. Yao, Z. Yuan, Y.G. Yao, G. Liu, C. Zhang, L. Liu, C. Chen, Increased GSNOR expression during aging impairs cognitive function and decreases S-nitrosation of CaMKIIalpha, J. Neurosci. 37 (2017) 9741–9758.
[25] S. Rizza, C. Cirotti, C. Montagna, S. Cardaci, C. Consales, M. Cozzolino, M.T. Carri, F. Cecconi, G. Filomeni, S-Nitrosoglutathione reductase plays opposite roles in SH-SY5Y models of Parkinson's disease and amyotrophic lateral sclerosis, Mediat. Inflamm. (2015), 536238.
[26] T. Gu, D. Yu, Y. Li, L. Xu, Y.L. Yao, Y.G. Yao, Establishment and characterization of an immortalized renal cell line of the Chinese tree shrew (Tupaia belangeri chinesis), Appl. Microbiol. Biotechnol. 103 (2019) 2171–2180.
[27] Q. Liu, L.Y. Su, C. Sun, L. Jiao, Y. Miao, M. Xu, R. Luo, X. Zuo, R. Zhou, P. Zheng, W. Xiong, T. Xue, Y.G. Yao, Melatonin alleviates morphine analgesic tolerance in mice by decreasing NLRP3 inflammasome activation, Redox Biol. 34 (2020), 101560.
[28] L.Y. Su, H. Li, L. Lv, Y.M. Feng, G.D. Li, R. Luo, H.J. Zhou, X.G. Lei, L. Ma, J.L. Li, L. Xu, X.T. Hu, Y.G. Yao, Melatonin attenuates MPTP-induced neurotoxicity via preventing CDK5-mediated autophagy and SNCA/alpha-synuclein aggregation, Autophagy 11 (2015) 1745–1759.
[29] S.R. Jaffrey, S.H. Snyder, The biotin switch method for the detection of S-nitrosylated proteins, Sci. STKE (2001) pl1, 2001.
[30] Y. Qin, A. Dey, Y. Daaka, Protein s-nitrosylation measurement, Methods Enzymol. 522 (2013) 409–425.
[31] Q.Z. Tuo, Z.Y. Liuyang, P. Lei, X. Yan, Y.P. Shentu, J.W. Liang, H. Zhou, L. Pei, Y. Xiong, T.Y. Hou, X.W. Zhou, Q. Wang, J.Z. Wang, X.C. Wang, R. Liu, Zinc induces CDK5 activation and neuronal death through CDK5-Tyr15 phosphorylation in ischemic stroke, Cell Death Dis. 9 (2018) 870.
[32] W. Wang, L. Shi, Y. Xie, C. Ma, W. Li, X. Su, S. Huang, R. Chen, Z. Zhu, Z. Mao, Y. Han, M. Li, SP600125, a new JNK inhibitor, protects dopaminergic neurons in the MPTP model of Parkinson's disease, Neurosci. Res. 48 (2004) 195–202.
[33] Y. Zhang, L. Qin, J. Xie, J. Li, C. Wang, Eupatilin prevents behavioral deficits and dopaminergic neuron degeneration in a Parkinson's disease mouse model, Life Sci. 253 (2020), 117745.
[34] W.W. Liu, S.Z. Wei, G.D. Huang, L.B. Liu, C. Gu, Y. Shen, X.H. Wang, S.T. Xia, A. M. Xie, L.F. Hu, F. Wang, C.F. Liu, BMAL1 regulation of microglia-mediated neuroinflammation in MPTP-induced Parkinson's disease mouse model, Faseb. J. 34 (2020) 6570–6581.
[35] H.S. Lim, B.C. Moon, J. Lee, G. Choi, G. Park, The insect molting hormone 20-hydroxyecdysone protects dopaminergic neurons against MPTP-induced neurotoxicity in a mouse model of Parkinson's disease, Free Radic. Biol. Med. 159 (2020) 23–36.
[36] E. Lee, I. Hwang, S. Park, S. Hong, B. Hwang, Y. Cho, J. Son, J.W. Yu, MPTP-driven NLRP3 inflammasome activation in microglia plays a central role in dopaminergic neurodegeneration, Cell Death Differ. 26 (2019) 213–228.
[37] R. Wu, H. Chen, J. Ma, Q. He, Q. Huang, Q. Liu, M. Li, Z. Yuan, c-Abl-p38alpha signaling plays an important role in MPTP-induced neuronal death, Cell Death Differ. 23 (2016) 542–552.
[38] D.J. Klionsky, A.K. Abdel-Aziz, S. Abdelfatah, M. Abdellatif, A. Abdoli, S. Abel, et al., Guidelines for the use and interpretation of assays for monitoring autophagy, Autophagy 17 (1) (2021) 1–382, fourth ed.
[39] P. Zhang, P.C. Yu, A.H. Tsang, Y. Chen, A.K. Fu, W.Y. Fu, K.K. Chung, N.Y. Ip, S-nitrosylation of cyclin-dependent kinase 5 (cdk5) regulates its kinase activity and dendrite growth during neuronal development, J. Neurosci. 30 (2010) 14366–14370.
[40] P. Zhang, W.Y. Fu, A.K. Fu, N.Y. Ip, S-nitrosylation-dependent proteasomal degradation restrains Cdk5 activity to regulate hippocampal synaptic strength, Nat. Commun. 6 (2015) 8665.
[41] J. Qu, T. Nakamura, G. Cao, E.A. Holland, S.R. McKercher, S.A. Lipton, S-nitrosylation activates Cdk5 and contributes to synaptic spine loss induced by beta-amyloid peptide, Proc. Natl. Acad. Sci. U. S. A. 108 (2011) 14330–14335.
[42] D.B. Colagiovanni, D.W. Drolet, E. Langlois-Forget, M.P. Piche, D. Looker, G. J. Rosenthal, A nonclinical safety and pharmacokinetic evaluation of N6022: a first-in-class S-nitrosoglutathione reductase inhibitor for the treatment of asthma, Regul. Toxicol. Pharmacol. 62 (2012) 115–124.
[43] L.S. Green, L.E. Chun, A.K. Patton, X. Sun, G.J. Rosenthal, J.P. Richards, Mechanism of inhibition for N6022, a first-in-class drug targeting S-nitrosoglutathione reductase, Biochemistry 51 (2012) 2157–2168.
[44] N. Saxena, J. Won, S. Choi, A.K. Singh, I. Singh, S-nitrosoglutathione reductase (GSNOR) inhibitor as an immune modulator in experimental autoimmune encephalomyelitis, Free Radic. Biol. Med. 121 (2018) 57–68.
[45] J. Kim, S.M.T. Islam, F. Qiao, A.K. Singh, M. Khan, J. Won, I. Singh, Regulation of B cell functions by S-nitrosoglutathione in the EAE model, Redox Biol. 45 (2021), 102053.
[46] M. Khan, P. Kumar, F. Qiao, S.M.T. Islam, A.K. Singh, J.S. Won, W. Feng, I. Singh, Targeting GSNOR for functional recovery in a middle-aged mouse model of stroke, Brain Res. 1741 (2020), 146879.
[47] C. Soto, S. Pritzkow, Protein misfolding, aggregation, and conformational strains in neurodegenerative diseases, Nat. Neurosci. 21 (2018) 1332–1340.
[48] J.L. Webb, B. Ravikumar, J. Atkins, J.N. Skepper, D.C. Rubinsztein, Alpha-Synuclein is degraded by both autophagy and the proteasome, J. Biol. Chem. 278 (2003) 25009–25013.
[49] I. Choi, Y. Zhang, S.P. Seegobin, M. Pruvost, Q. Wang, K. Purtell, B. Zhang, Z. Yue, Microglia clear neuron-released alpha-synuclein via selective autophagy and prevent neurodegeneration, Nat. Commun. 11 (2020) 1386.
[50] S.L. Wynia-Smith, B.C. Smith, Nitrosothiol formation and S-nitrosation signaling through nitric oxide synthases, Nitric Oxide 63 (2017) 52–60.
[51] T. Nakamura, S.A. Lipton, Protein S-nitrosylation as a therapeutic target for neurodegenerative diseases, Trends Pharmacol. Sci. 37 (2016) 73–84.
[52] L.G. Que, Z. Yang, J.S. Stamler, N.L. Lugogo, M. Kraft, S-nitrosoglutathione reductase: an important regulator in human asthma, Am. J. Respir. Crit. Care Med. 180 (2009) 226–231.
[53] K.E. Hatzistergos, E.C. Paulino, R.A. Dulce, L.M. Takeuchi, M.A. Bellio, S. Kulandavelu, Y. Cao, W. Balkan, R.M. Kanashiro-Takeuchi, J.M. Hare, S-nitrosoglutathione reductase deficiency enhances the proliferative expansion of adult heart progenitors and myocytes post myocardial infarction, J. Am. Heart Assoc. 4 (2015).
[54] R.E. Elphinstone, R. Besla, E.A. Shikatani, Z. Lu, A. Hausladen, M. Davies, C. S. Robbins, M. Husain, J.S. Stamler, K.C. Kain, S-Nitrosoglutathione reductase deficiency confers improved survival and neurological outcome in experimental cerebral malaria, Infect. Immun. 85 (2017).
[55] S. Rizza, S. Cardaci, C. Montagna, G. Di Giacomo, D. De Zio, M. Bordi, E. Maiani, S. Campello, A. Borreca, A.A. Puca, J.S. Stamler, F. Cecconi, G. Filomeni, S-nitrosylation drives cell senescence and aging in mammals by controlling mitochondrial dynamics and mitophagy, Proc. Natl. Acad. Sci. U. S. A. 115 (2018) E3388–E3397.
[56] S. Rizza, G. Filomeni, Denitrosylate and live longer: how ADH5/GSNOR links mitophagy to aging, Autophagy 14 (2018) 1285–1287.
[57] B. Levine, G. Kroemer, Autophagy in the pathogenesis of disease, Cell 132 (2008) 27–42.
[58] M. Xilouri, O.R. Brekk, L. Stefanis, Autophagy and alpha-synuclein: relevance to Parkinson's disease and related synucleopathies, Mov. Disord. 31 (2016) 178–192.
[59] X. Hou, J.O. Watzlawik, F.C. Fiesel, W. Springer, Autophagy in Parkinson's disease, J. Mol. Biol. 432 (2020) 2651–2672.
[60] A.S. Wong, R.H. Lee, A.Y. Cheung, P.K. Yeung, S.K. Chung, Z.H. Cheung, N.Y. Ip, Cdk5-mediated phosphorylation of endophilin B1 is required for induced autophagy in models of Parkinson's disease, Nat. Cell Biol. 13 (2011) 568–579.
[61] L. Zhu, C. Zhang, Q. Liu, PTEN S-nitrosylation by NOS1 inhibits autophagy in NPC cells, Cell Death Dis. 10 (2019) 306.
[62] C. Wright, A.K. Iyer, Y. Kulkarni, N. Azad, S-nitrosylation of bcl-2 negatively affects autophagy in lung epithelial cells, J. Cell. Biochem. 117 (2016) 521–532.
[63] S. Sarkar, V.I. Korolchuk, M. Renna, S. Imarisio, A. Fleming, A. Williams, M. Garcia-Arencibia, C. Rose, S. Luo, B.R. Underwood, G. Kroemer, C.J. O'Kane, D. C. Rubinsztein, Complex inhibitory effects of nitric oxide on autophagy, Mol. Cell 43 (2011) 19–32.
[64] Y. Li, Y. Zhang, L. Wang, P. Wang, Y. Xue, X. Li, X. Qiao, X. Zhang, T. Xu, G. Liu, P. Li, C. Chen, Autophagy impairment mediated by S-nitrosation of ATG4B leads to neurotoxicity in response to hyperglycemia, Autophagy 13 (2017) 1145–1160.
[65] D. Qu, J. Rashidian, M.P. Mount, H. Aleyasin, M. Parsanejad, A. Lira, E. Haque, Y. Zhang, S. Callaghan, M. Daigle, M.W. Rousseaux, R.S. Slack, P.R. Albert, I. Vincent, J.M. Woulfe, D.S. Park, Role of Cdk5-mediated phosphorylation of Prx2 in MPTP toxicity and Parkinson's disease, Neuron 55 (2007) 37–52.
[66] J. Zhou, H. Li, X. Li, G. Zhang, Y. Niu, Z. Yuan, K. Herrup, Y.W. Zhang, G. Bu, H. Xu, J. Zhang, The roles of Cdk5-mediated subcellular localization of FOXO1 in neuronal death, J. Neurosci. 35 (2015) 2624–2635.
[67] Q. Wang, F. Jiao, P. Zhang, J. Yan, Z. Zhang, F. He, Q. Zhang, Z. Lv, X. Peng, H. Cai, B. Tian, CDK5-mediated phosphorylation-dependent ubiquitination and degradation of E3 ubiquitin ligases GP78 accelerates neuronal death in Parkinson's disease, Mol. Neurobiol. 55 (2018) 3709–3717.
[68] J. Zhou, H.M. Chow, Y. Liu, D. Wu, M. Shi, J. Li, L. Wen, Y. Gao, G. Chen, K. Zhuang, H. Lin, G. Zhang, W. Xie, H. Li, L. Leng, M. Wang, N. Zheng, H. Sun, Y. Zhao, Y. Zhang, M. Xue, T.Y. Huang, G. Bu, H. Xu, Z. Yuan, K. Herrup, J. Zhang, Cyclin-dependent kinase 5-dependent BAG3 degradation modulates synaptic protein turnover, Biol. Psychiatr. 87 (2020) 756–769.
[69] P.D. Smith, S.J. Crocker, V. Jackson-Lewis, K.L. Jordan-Sciutto, S. Hayley, M. P. Mount, M.J. O'Hare, S. Callaghan, R.S. Slack, S. Przedborski, H. Anisman, D. S. Park, Cyclin-dependent kinase 5 is a mediator of dopaminergic neuron loss in a mouse model of Parkinson's disease, Proc. Natl. Acad. Sci. U. S. A. 100 (2003) 13650–13655.
[70] L.R. Zukerberg, G.N. Patrick, M. Nikolic, S. Humbert, C.L. Wu, L.M. Lanier, F. B. Gertler, M. Vidal, R.A. Van Etten, L.H. Tsai, Cables links Cdk5 and c-Abl and facilitates Cdk5 tyrosine phosphorylation, kinase upregulation, and neurite outgrowth, Neuron 26 (2000) 633–646.
[71] P. Sharma, M. Sharma, N.D. Amin, R.W. Albers, H.C. Pant, Regulation of cyclin-dependent kinase 5 catalytic activity by phosphorylation, Proc. Natl. Acad. Sci. U. S. A. 96 (1999) 11156–11160.

Supplementary Material

GSNOR deficiency attenuates MPTP-induced neurotoxicity and autophagy by facilitating CDK5 *S*-nitrosation in a mouse model of Parkinson's disease

Lijin Jiao [1, 2, 5], Ling-Yan Su [1, 2, 5], Qianjin Liu [1, 2, 5], Rongcan Luo[1, 2], Xinhua Qiao [3], Ting Xie [3], Lu-Xiu Yang[1], Chang Chen [3], Yong-Gang Yao [1, 2, 4, *]

Supporting information Table S1-S3

Supporting information Figure S1-S6

Table S1. Antibodies and chemicals used in this study

Antibody	Source	Catalog no.	Western blot	IHC
Primary antibody				
Rabbit polyclonal anti-GSNOR	Abcam	ab175406	1:1000	-
Mouse monoclonal anti-CDK5	Santa Cruz Biotechnology	sc-6247	1:1000	-
Rabbit monoclonal anti-SQSTM1/P62	Cell Signaling Technology	8025T	1:1000	-
Rabbit polyclonal anti-MAP1LC3/LC3	Proteintech	4600-1-AP	1:1000	-
Rabbit polyclonal anti-TH	Merck Millipore	AB152	-	1:500
Rabbit monoclonal anti-Histone H1	Abcam	ab134914	1:1000	-
Mouse monoclonal anti-phospho-histone H1	Millipore	05-1324	1:1000	-
Mouse monoclonal anti-Flag	Abmart	TT0003	1:1000	-
Mouse monoclonal anti-Myc	Invitrogen	R950-25	1:1000	-
Mouse monoclonal anti-tubulin	EnoGene	E1C601	1:10000	-
Mouse monoclonal anti-GAPDH	Proteintech	60004-1-Ig	1:10000	-
Mouse monoclonal anti-ACTB	Beijing Zhong Shan-Golden Bridge Biological Technology CO., LTD	TA-09	1:10000	-
Secondary antibody				
Peroxidase-conjugated anti-rabbit antibody	KPL	474-1516	1:10000	-
Peroxidase-conjugated anti-mouse antibody	KPL	474-1806	1:10000	-
Chemicals				
MPTP	Sigma-Aldrich	M0896	-	-
MPP^+	Sigma-Aldrich	D048-100	-	-
S-nitrosoglutathione (GSNO)	Santa Cruz	sc-200349A	-	-
Glutathione (GSH)	Selleckchem	S4606	-	-
N6022	TargetMol	T6901	-	-
Methyl methanethiosulfonate (MMTS)	Sigma-Aldrich	208795-1G	-	-
Biotin-HPDP	Glpbio	GC11037-100	-	-
Recombinant Human Histone H1 protein	Abcam	ab198676	-	-
4', 6-diamidino-2-phenylindole (DAPI)	Roche	10236276001	-	-
Assay Dilution Buffer 5X	Millipore	20-145	-	-
Dimethylsulfoxide (DMSO)	Beyotime	ST038	-	-

IHC - Immunohistochemistry

Table S2. Primers used in this study

Gene	Name	Primer sequence (5' - 3')	Application
Cdk5	MYC-CDK5 Rat-F	ccggaagatctgagctcgagATGCAGAAATACGAGAAACTGG	PCR for constructing pCS2-N-Myc-CDK5 using
	MYC-CDK5 Rat-R	tatagttctagaggctcgagCTACGGGGGACAGAAGTCAGAG	pCS-myc-N vector
	CDK5-C53S-Rat-F	CGGGAGATCTCTCTACTCAAA	PCR for constructing pCS2-N-Myc-CDK5-C53S
	CDK5-C53S-Rat-R	TTTGAGTAGAGAGATCTCCCG	using pCS-myc-N-CDK5 vector
	CDK5-C83S-Rat-F	TTTGAGTTCTCTGATCAGGAC	PCR for constructing pCS2-N-Myc-CDK5-C83S
	CDK5-C83S-Rat-R	GTCCTGATCAGAGAACTCAAA	using pCS-myc-N-CDK5 vector
	CDK5-C94S-Rat-F	TTTGACAGCTCCAATGGTGAC	PCR for constructing pCS2-N-Myc-CDK5-C94S
	CDK5-C94S-Rat-R	GTCACCATTGGAGCTGTCAAA	using pCS-myc-N-CDK5 vector
	CDK5-C117S-Rat-F	CTGGGATTCTCTCACAGCCGT	PCR for constructing pCS2-N-Myc-CDK5-C117S
	CDK5-C117S-Rat-R	ACGGCTGTGAGAGAATCCCAG	using pCS-myc-N-CDK5 vector
	CDK5-C157S-Rat-F	CCAGTCCGCTCCTACTCTGCT	PCR for constructing pCS2-N-Myc-CDK5-C157S
	CDK5-C157S-Rat-R	AGCAGAGTAGGAGCGGACTGG	using pCS-myc-N-CDK5 vector
	CDK5-C190S-Rat-F	TCAGCCGGCTCCATCTTTGCA	PCR for constructing pCS2-N-Myc-CDK5-C190S
	CDK5-C190S-Rat-R	TGCAAAGATGGAGCCGGCTGA	using pCS-myc-N-CDK5 vector
	CDK5-C269S-Rat-F	CTGTTGAAGTCTAACCCAGTG	PCR for constructing pCS2-N-Myc-CDK5-C269S
	CDK5-C269S-Rat-R	CACTGGGTTAGACTTCAACAG	using pCS-myc-N-CDK5 vector
	CDK5-C290S-Rat-F	TCTGACTTCTCTCCCCCGTAG	PCR for constructing pCS2-N-Myc-CDK5-C290S
	CDK5-C290S-Rat-R	CTACGGGGGAGAGAAGTCAGAG	using pCS-myc-N-CDK5 vector
Gsnor	Gsnor-sgRNA-F	CACCGGTGTAAGGCTGCAGTCGCC	For constructing CRISPR/Cas9 vector for GSNOR
	Gsnor-sgRNA-R	AAACGGCGACTGCAGCCTTACACC	knockout using pX330-T7 vector
	Gsnor-F	TTGCTCCACCATGTATCGA	PCR and sequencing for the *Gsnor* gene region
	Gsnor-R	CCTTCTCCCACAATGCTTA	spanning the sgRNA targeting site

Note: the nucleotides in the lowercase stand for homologous sequence, and the underlined nucleotides were responsible for introducing point mutation.

Table S3. Buffer used in the biotin switch assays

Buffer name	Composition of buffer
HEN buffer	250 mM HEPES-NaOH [pH 7.7], 1 mM EDTA and 0.1 mM neocuproine
Blocking buffer	250 mM HEPES-NaOH [pH 7.7], 1 mM EDTA, 0.1 mM neocuproine, 2.5% SDS, and 20 mM MMTS
HENS buffer	250 mM HEPES-NaOH [pH 7.7], 1 mM EDTA, 0.1 mM neocuproine, and 1% SDS
Neutralization buffer	20 mM HEPES-NaOH [pH 7.7], 100 mM NaCl, 1 mM EDTA, and 0.5% Triton X-100
Elution buffer	20 mM HEPES-NaOH [pH 7.7], 100 mM NaCl, 1 mM EDTA, and 100 mM β-Mercaptoethanol

Note: the compositions of these buffers were taken from [1].

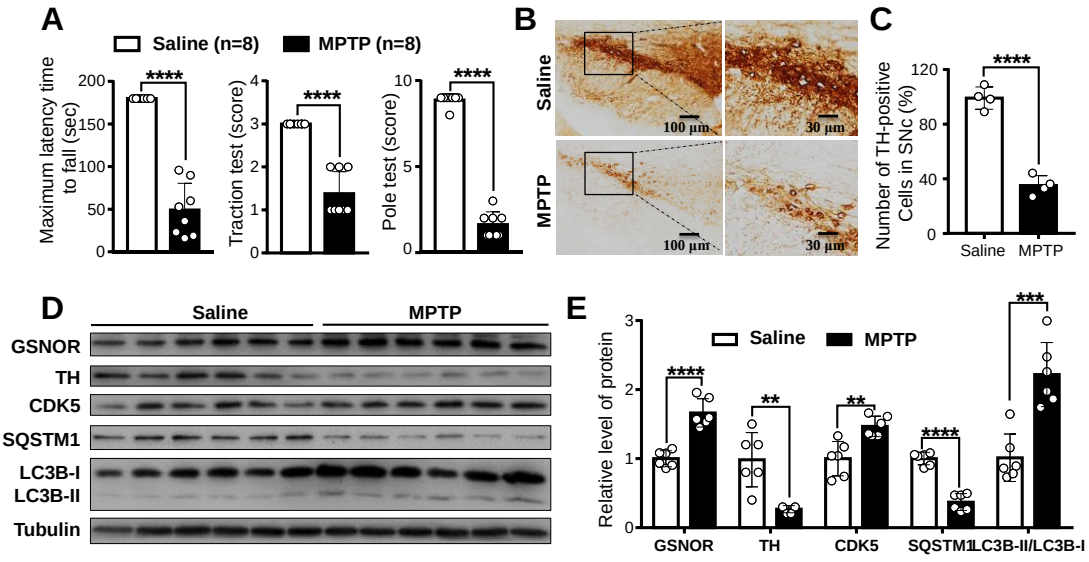

Fig. S1. MPTP induced CDK5-mediated autophagy and GSNOR upregulation in MPTP-induced PD mouse model.

(**A**) MPTP-treated mice (MPTP group) had a significant decrease of performance as compared to untreated mice (Saline group). Wild type (WT) mice were divided into Saline group and MPTP group, then were subjected to the behavioral tests on Day 0 (Baseline). Animals were injected with MPTP or saline daily for 2 weeks, and received the behavioral tests on Day 15 (Test).

(**B**) Representative TH immunoreactivity of the SNc region in mice (n = 4 mice per group).

(**C**) Quantification of the numbers of TH-positive cells in (**B**). A single dot in the bar represents the average count for TH positive cells in at least five slices of each animal.

(**D**-**E**) Protein levels of GSNOR, TH, CDK5, SQSTM1, LC3B-II and LC3B-I in striatal tissues from mice (n = 6 mice per group) in (**A**). Tubulin was used as loading control.

Data are normalized to the mice without MPTP treatment (Saline group) and are presented as mean ± SD. **, $P < 0.01$; ***, $P < 0.001$; ****, $P < 0.0001$; two-tailed unpaired Student's *t* test.

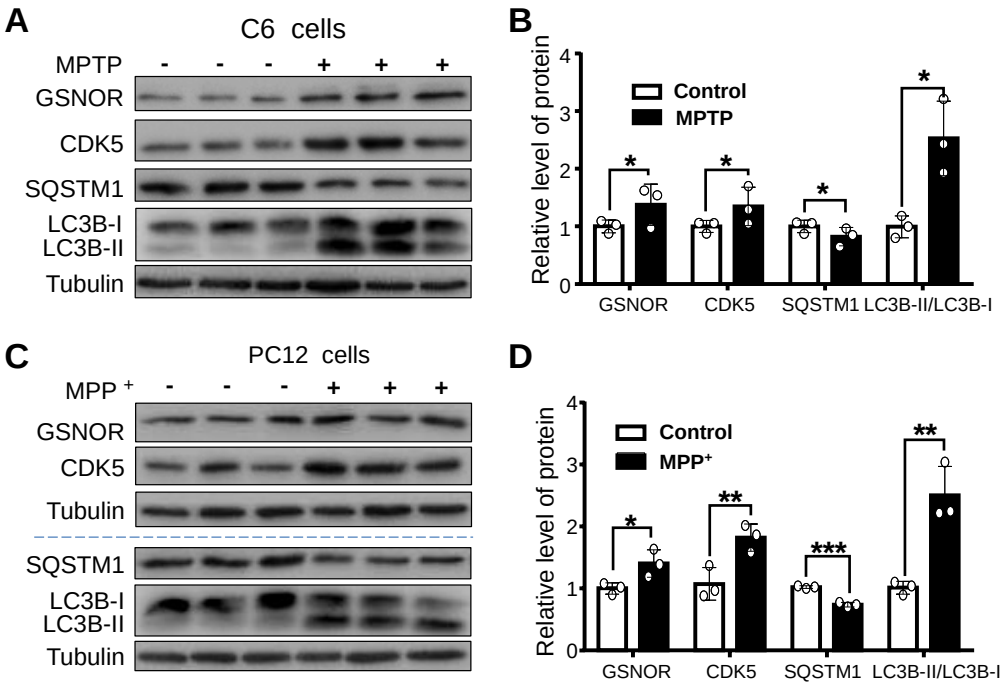

Fig. S2. Upregulation of GSNOR and CDK5-mediated autophagy in C6 with or without MPTP treatment and PC12 cells with or without MPP^+ treatment.

(**A**) Protein levels of GSNOR, CDK5, SQSTM1, LC3B-II and LC3B-I in wild-type C6 cells with or without MPTP treatment.

(**B**) Quantification of relative protein levels and LC3B-II:LC3B-I ratio in (**A**).

(**C**) Protein levels of GSNOR, CDK5, SQSTM1, LC3B-II and LC3B-I in wild-type PC12 cells with or without MPP^+ treatment.

(**D**) Quantification of relative protein levels and LC3B-II:LC3B-I ratio in (**C**).

Tubulin was used as loading control in (A) and (C). Shown results are representative of three independent experiments with similar results. Data are normalized to cells without treatment (Control) and values are mean ± SD. *, $P < 0.05$; **, $P < 0.01$; ***, $P < 0.001$; two-tailed unpaired Student's *t* test.

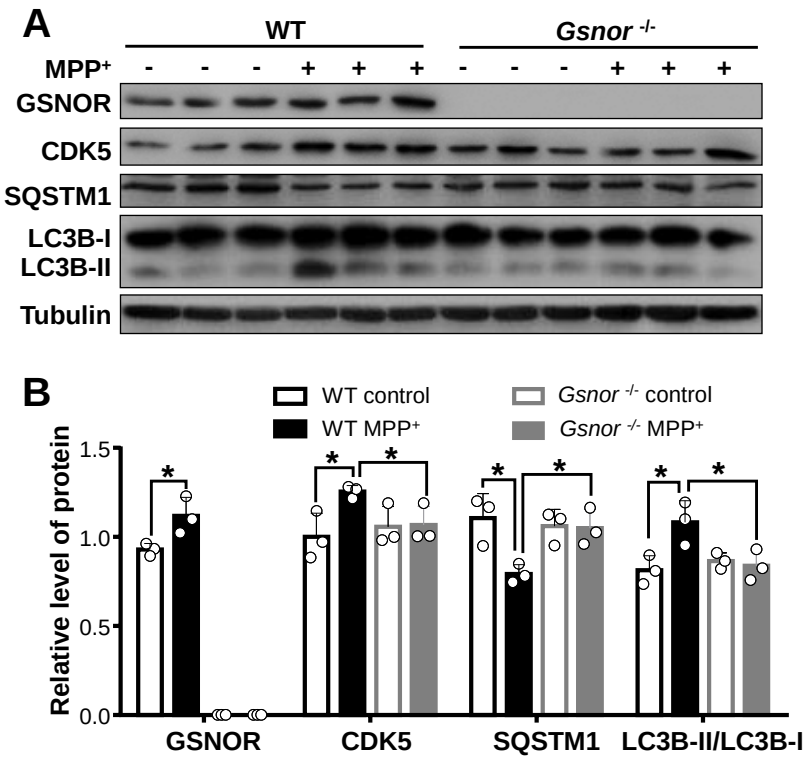

Fig. S3. GSNOR deficiency impaired MPTP-induced CDK5-mediated autophagy in PC12 cells. (**A**) Protein levels of GSNOR, CDK5, SQSTM1, LC3B-II and LC3B-I in wild-type (WT) and GSNOR knockout (*Gsnor*$^{-/-}$) PC12 cells with or without MPP$^+$ treatment. Tubulin was used as loading control.

(**B**) Quantification of relative protein levels and LC3B-II:LC3B-I ratio in (**A**). Shown results are representative of three independent experiments with similar results. Data are normalized to WT PC12 cells without MPP$^+$ treatment (WT control) and values are mean ± SD. *, $P < 0.05$; two-way ANOVA with the Tukey's post-hoc test.

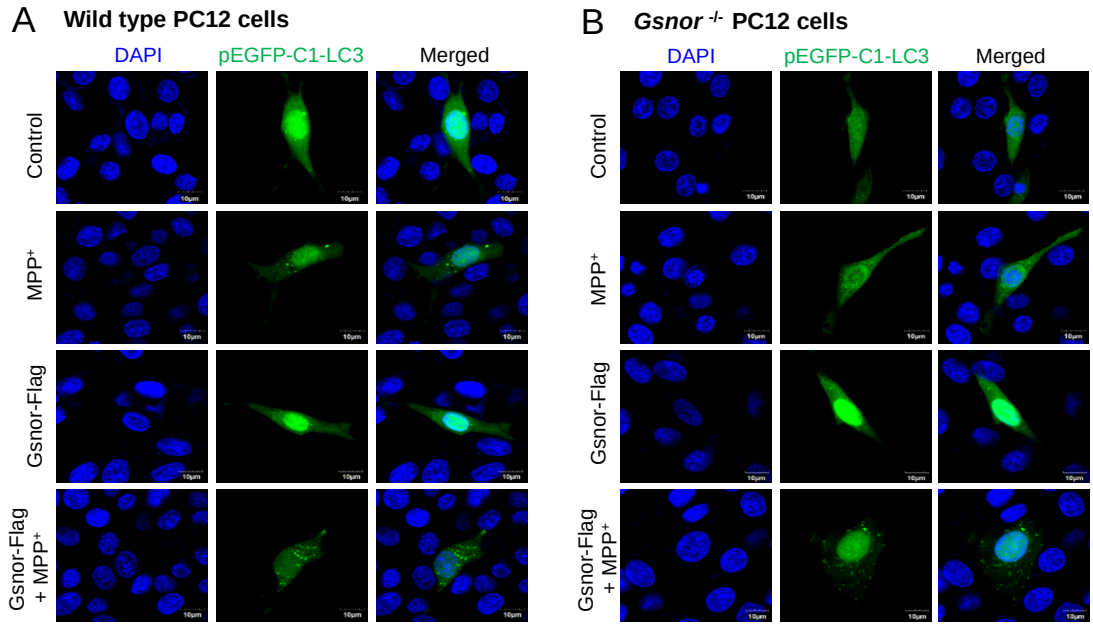

Fig. S4. GSNOR deficiency alleviates MPP^+-induced CDK5-mediated autophagy in PC12 cells. (**A-B**) Immunofluorescence assays for EGFP-LC3 puncta in wild type PC12 cells (**A**) and *Gsnor*$^{-/-}$ PC12 cells (**B**) overexpressing empty vector and GSNOR, with or without MPP^+ treatment. Wild type and *Gsnor*$^{-/-}$ PC12 cells were co-transfected with empty vector (Vector-flag) and N-terminally tagged pEGFP-C1-LC3 or GSNOR (Gsnor-Flag) and N-terminally tagged pEGFP-C1-LC3 for 24 h, then received MPP^+ (100 μM) treatment for another 24 h before the immunofluorescence assay.

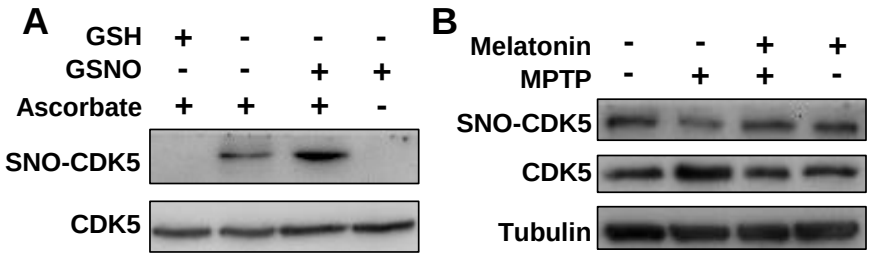

Fig. S5. *S*-nitrosation of CDK5 in C6 cells. (A) Cell lysates of C6 cells were incubated with GSNO (500 μM) or GSH (500 μM) at room temperature for 30 min, then were subjected to biotin switch assay in the presence or absence of ascorbate (10 mM). The biotinylated proteins were immunoprecipitated (IP) with streptavidin-agarose beads, followed by Western blot analysis for CDK5.

(B) MPTP treatment decreased the S-nitrosation of CDK5 in C6 cells and this effect could be rescued by a pretreatment with melatonin. C6 cells were pretreated with melatonin (100 μM) for 30 min, followed by a treatment with MPTP (500 μM) for 24 h. Cell lysates of C6 cells were harvested for the biotin switch assays and the biotinylated proteins were detected as in (A). Tubulin was used as loading control.

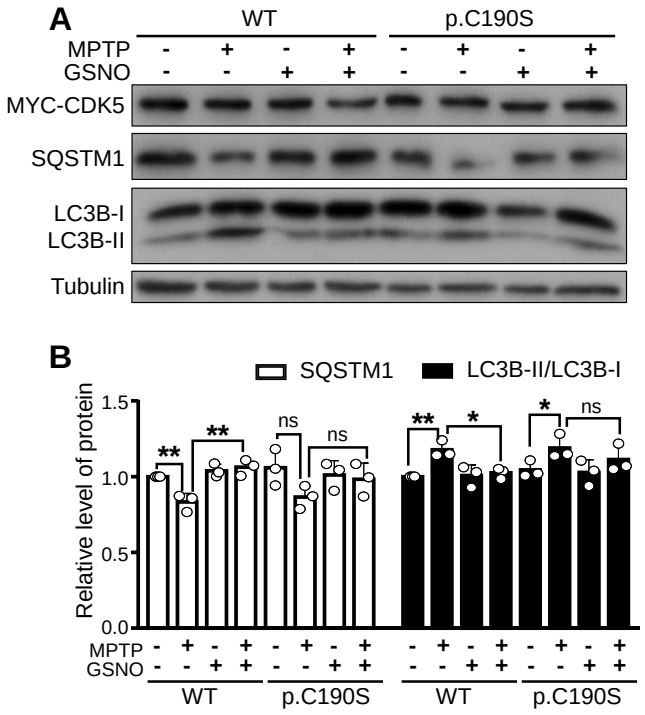

Fig. S6. S-nitrosation of CDK5 at Cys190 did not affect MPTP-induced autophagy.

(**A**) Effect of overexpression of CDK5 cysteine mutant p.C190S on CDK5-mediated autophagy in C6 cells. Cells were transfected with expression vector of wild type CDK5 (WT) or CDK5 cysteine mutant p.C190S (p.C190S) for 24 h, then received a pretreatment with or without GSNO (500 μM) for 30 min before the treatment with or without MPTP (500 μM). Tubulin was used as loading control.

(**B**) Quantification of protein level of SQSTM1 and LC3B-II:LC3B-I ratio in (**A**). Shown data are representative of three independent experiments with similar results. Data are normalized to WT C6 cells transfected with expression vector of wild type CDK5 (WT) without GSNO and MPTP treatment. Values are present as mean ± SD. ns, not significant; *, $P < 0.05$; **, $P < 0.01$; one-way ANOVA with the Tukey's post-hoc test.

References

[1] S.R. Jaffrey, S.H. Snyder, The biotin switch method for the detection of S-nitrosylated proteins, Sci STKE 2001 (2001) pl1.

The entire images of Western blot for Figure 1D.

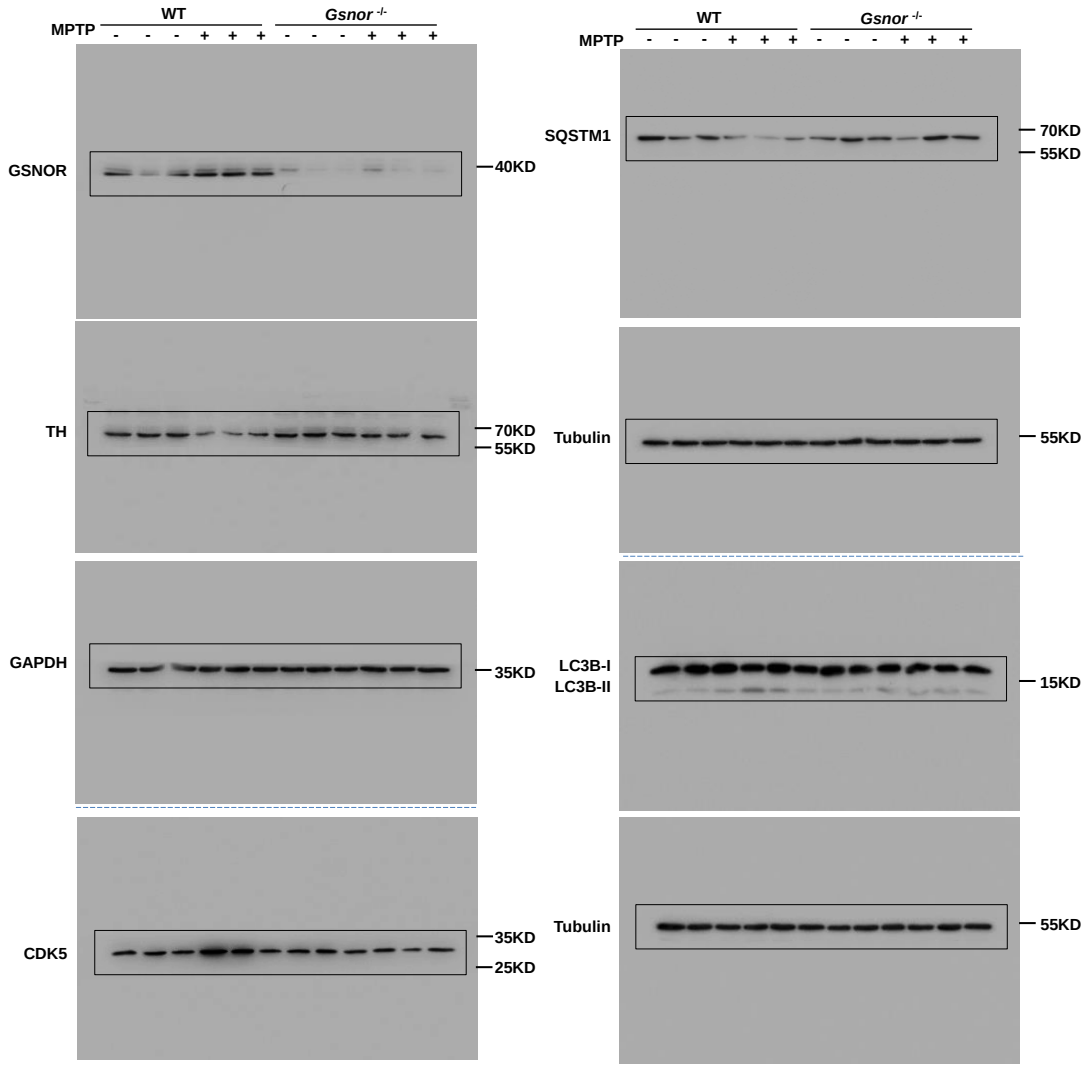

The entire images of Western blot for Figures 2A and 2C.

Figure 2A

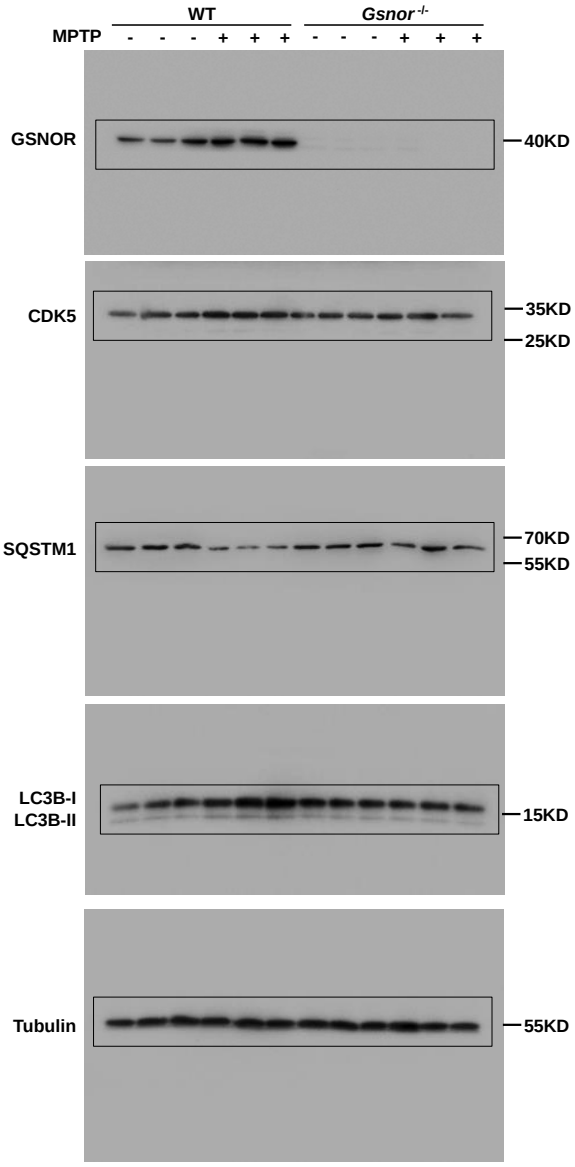

Figure 2C

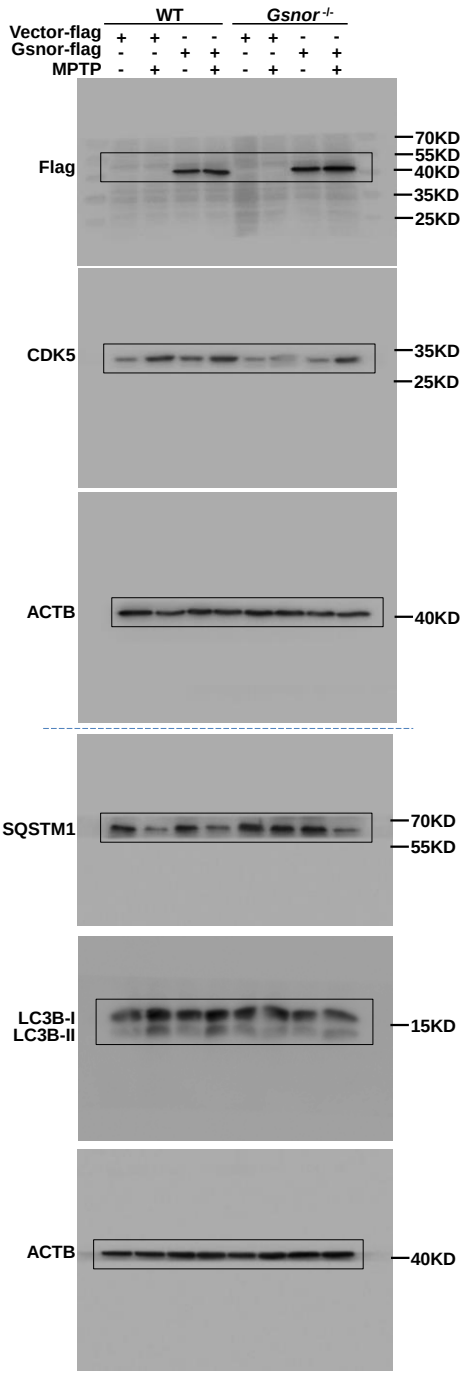

The entire images of Western blot for Figures 3A, 3C, 3E, and 3G.

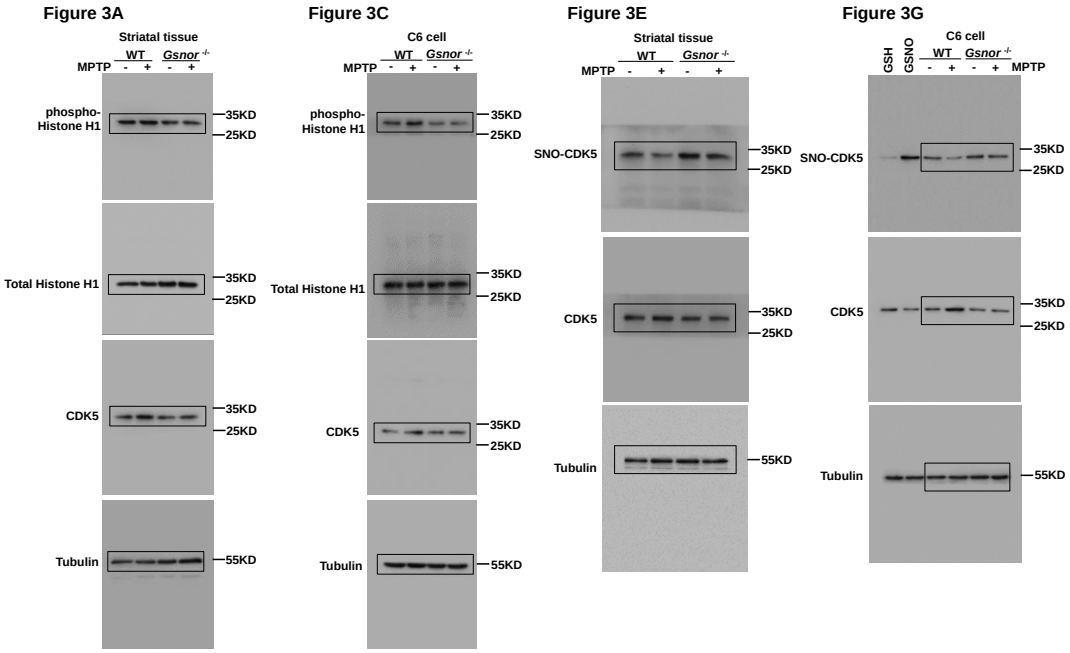

The entire images of Western blot for Figures 4B, 4D, and 4F.

Figure 4B

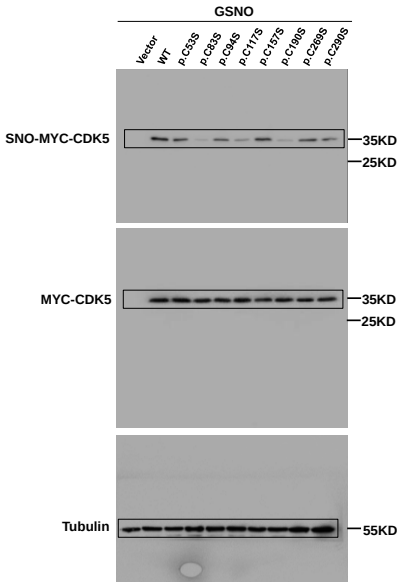

Figure 4D

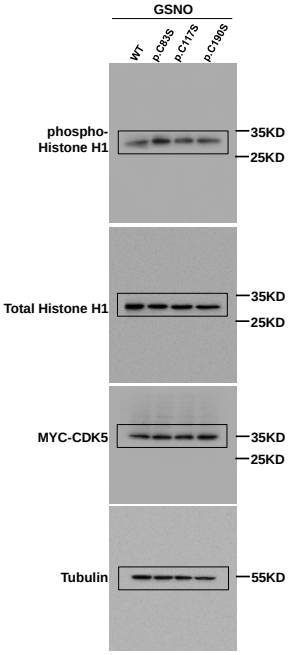

Figure 4F

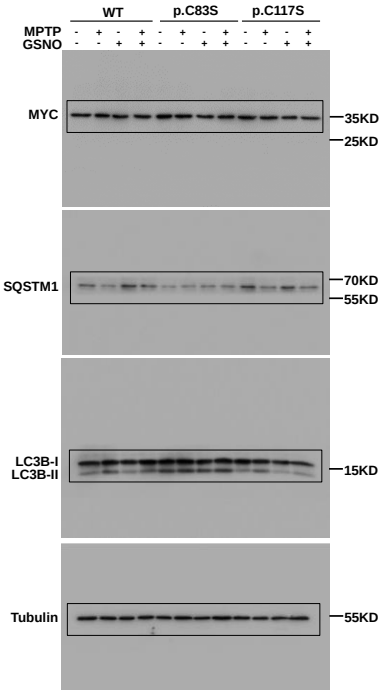

The entire images of Western blot for Figures 5B, 5D, and 5F.

Figure 5B

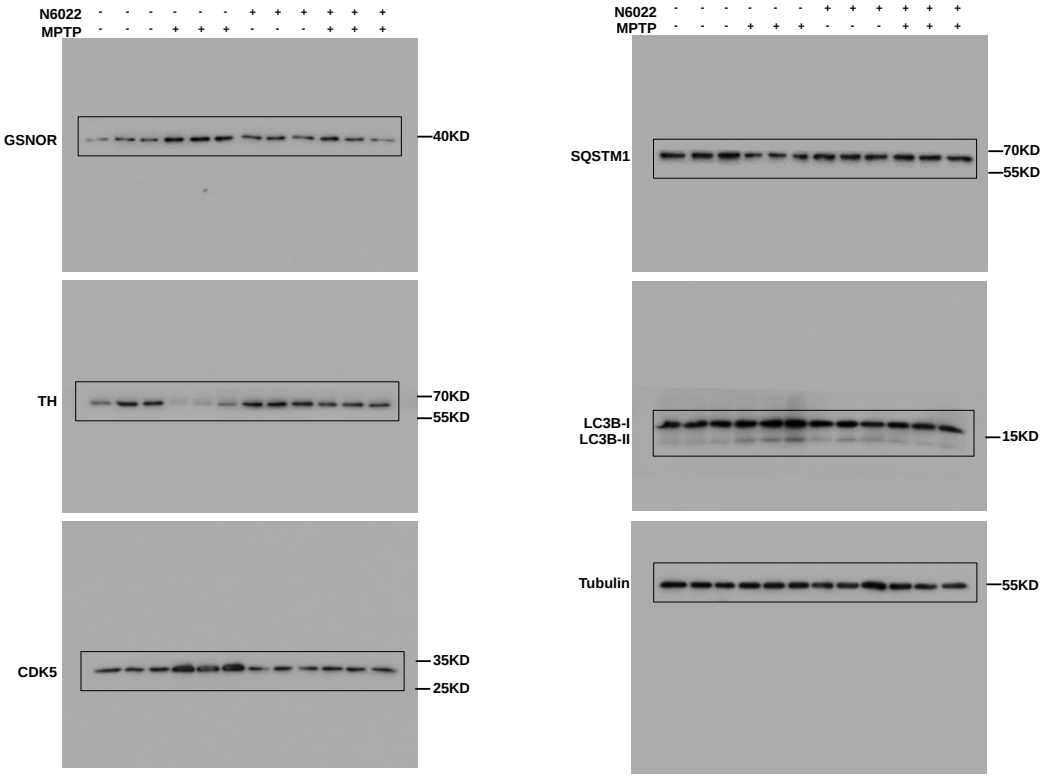

Figure 5D

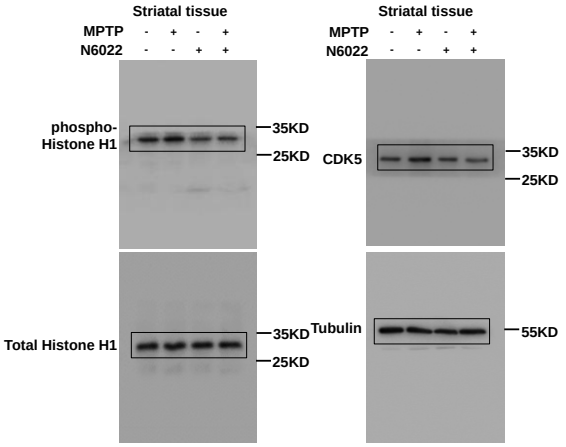

Figure 5F

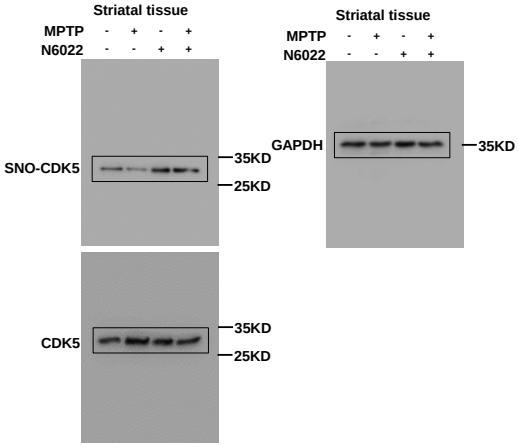

The entire images of Western blot for Figure S1D

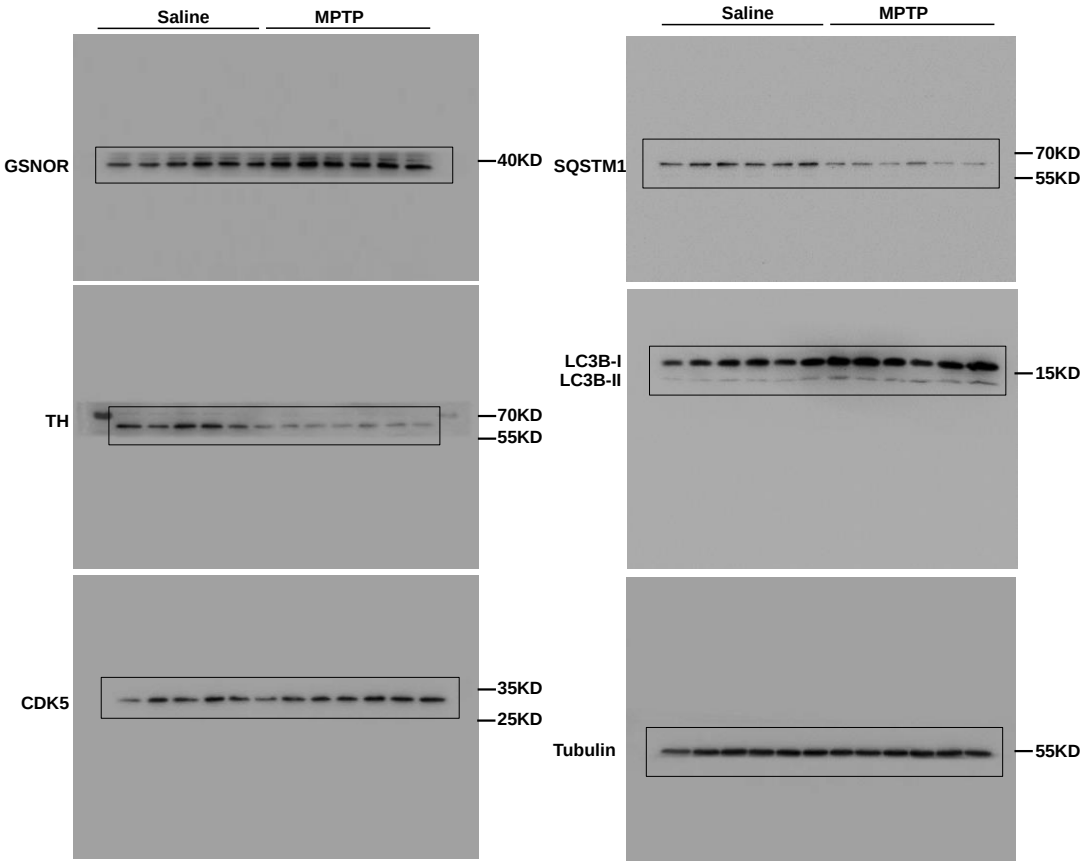

The entire images of Western blot for Figures S2A and S2C

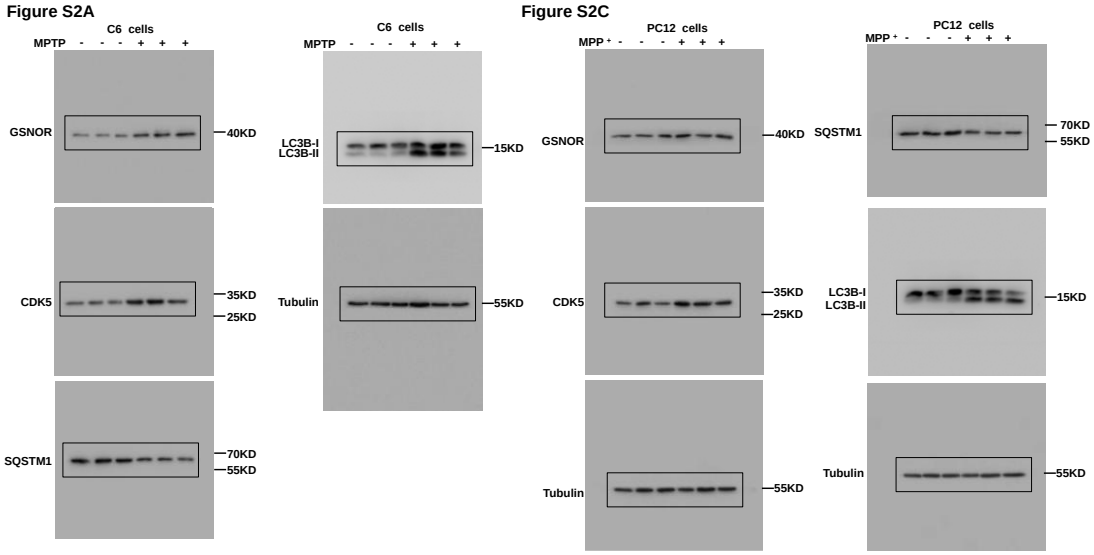

The entire images of Western blot for Figure S3A

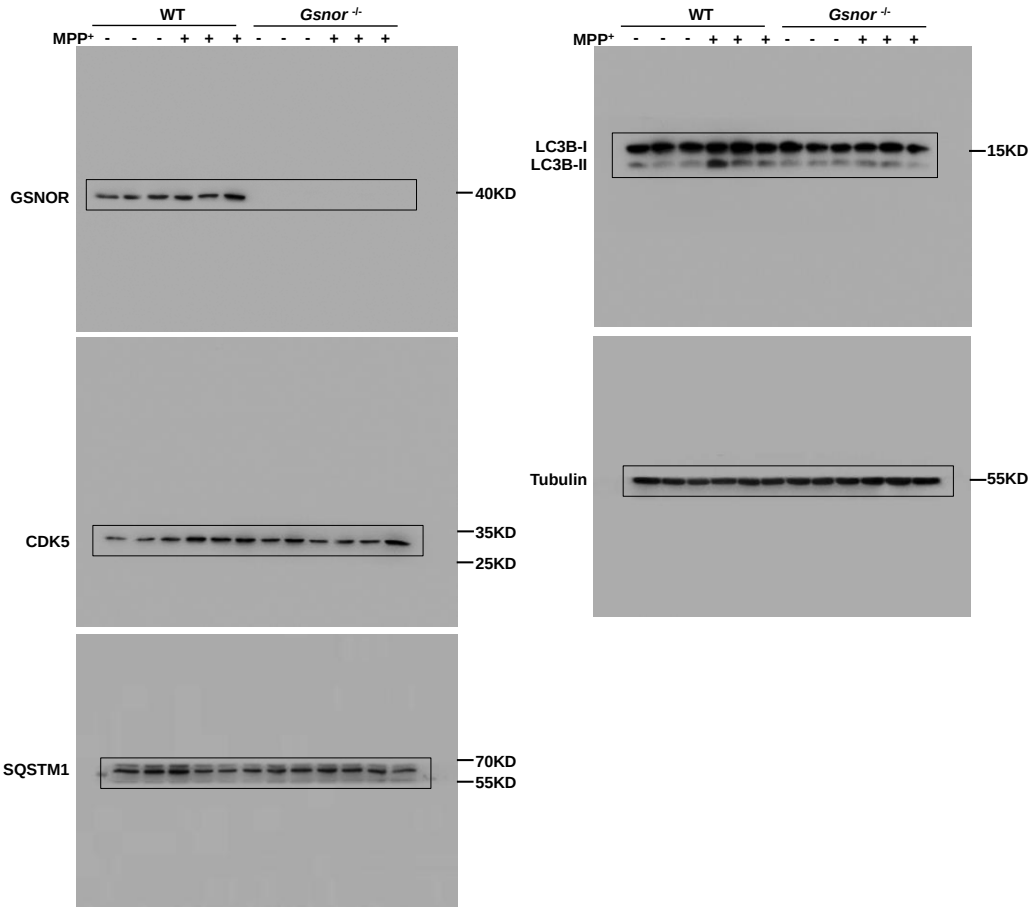

The entire images of Western blot for Figures S5A, S5B and S6